

Guidance for twisted particle filter: a continuous-time perspective

Jianfeng Lu^{*a} and Yuliang Wang^{†b}

^aDepartment of Mathematics, Department of Physics, Department of Chemistry, Duke University, Durham, NC 27708, USA.

^bSchool of Mathematical Sciences, Institute of Natural Sciences, Shanghai Jiao Tong University, Shanghai, 200240, P.R.China.

Abstract

The particle filter (PF), also known as the sequential Monte Carlo (SMC), is designed to approximate high-dimensional probability distributions and their normalizing constants in the discrete-time setting. To reduce the variance of the Monte Carlo approximation, several twisted particle filters (TPF) have been proposed by researchers, where one chooses or learns a twisting function that modifies the Markov transition kernel. In this paper, we study the TPF from a continuous-time perspective. Under suitable settings, we show that the discrete-time model converges to a continuous-time limit, which can be solved through a series of well-studied control-based importance sampling algorithms. This discrete-continuous connection allows the design of new TPF algorithms inspired by established continuous-time algorithms. As a concrete example, guided by existing importance sampling algorithms in the continuous-time setting, we propose a novel algorithm called “Twisted-Path Particle Filter” (TPPF), where the twist function, parameterized by neural networks, minimizes specific KL-divergence between path measures. Some numerical experiments are given to illustrate the capability of the proposed algorithm.

Keywords: twisted particle filter, sequential Monte Carlo, stochastic optimal control, importance sampling, neural network

1 Introduction

The particle filter (PF), or the sequential Monte Carlo (SMC), has found a wide range of applications in various areas such as computational statistics and machine learning. It has received increasing popularity when dealing with tasks including statistical inference problems for state space models [18, 55, 46, 52] and complex static models [6, 10], capability and safety techniques in large language models (LLM) [69, 57, 70, 67], to name a few. Generally, the particle filter involves the simulation of an artificial particle system over time, particularly suited for estimating statistical quantities of the following form via Monte Carlo:

$$Z = \mathbb{E} \left[\prod_{k=0}^n g_k(X_k) \right], \quad (1.1)$$

where g_k ($0 \leq k \leq n$) are deterministic functions and $(X_k)_{k=0}^n$ is a discrete-time Markov chain in \mathbb{R}^d with transition kernel $P(x, dy)$. The simplest and most classical algorithm to solve (1.1) is the bootstrap particle algorithm (BPF) proposed by Gordon, Salmond, and Smith in 1993 [25] (see Algorithm 1 below). However, to achieve a desired level of precision,

*E-mail: jianfeng@math.duke.edu

†Email: YuliangWang_math@sjtu.edu.cn

the required sample number N in the Monte Carlo approximation can be rather demanding, since the variance of $\prod_{k=0}^n g_k(X_k)$ can be large. In order to reduce the variance, various “twisted” particle filters have been developed [33, 26, 3, 63, 5, 67, 41, 40]. The general idea of the twisted particle filter (TPF) is as follows: Find a suitable (positive) twisting function $\varphi(k, x)$ ($1 \leq k \leq n$, $x \in \mathbb{R}^d$), run the twisted Markov chain X^φ with the transition kernel $P_k^\varphi(x, \cdot) \sim \varphi(k, \cdot)P(x, \cdot)$ at the k -th step, and modify the function sequence g_k according to φ (denoted by g_k^φ) (see more details in (2.5)–(2.7) below). The twisted model wants to achieve:

- (1) The statistical quantity Z is preserved (i.e. $\mathbb{E}[\prod_{k=0}^n g_k(X_k)] = \mathbb{E}[\prod_{k=0}^n g_k^\varphi(X_k^\varphi)]$)
- (2) The variance of $\prod_{k=0}^n g_k^\varphi(X_k^\varphi)$ is significantly reduced with a suitable choice of φ .

Notably, this approach is exactly the methodology of the importance sampling [38, 24, 1] via a change of measure for discrete path measures, and the key step in constructing a twisted model is seeking the optimal twisting function φ to minimize the variance above. In fact, most existing TPF algorithms adopt the “look ahead” strategies when constructing or learning the twisting function φ (see [52, 33, 26] for instance), due to the expression of the optimal twisting function (see (2.11) and (2.12) below).

Similar minimization problems are well-studied in the continuous-time setting, where importance sampling task can be recasted into a stochastic optimal control problem. A fruitful line of research has established several algorithms for the problem [32, 30, 53, 54]. Such control-based algorithms have wide range of applications in various areas including molecular dynamics [31, 53], mathematical finance [22, 23], etc. In this paper, for some continuous-time Markov process $(X_t)_{t \geq 0}$ and deterministic functions h, g , we are particularly interested in the target quantity of the form

$$Z = \mathbb{E} \left[\exp \left(\int_0^T h(s, X_s) ds \right) g(X_T) \right], \quad (1.2)$$

and the corresponding control-based importance sampling algorithms to reduce the variance of $\exp \left(\int_0^T h(s, X_s) ds \right) g(X_T)$. See more details in Section 2.2.

Remarkably, although the discrete-time particle filter and the continuous-time control-based importance sampling are typically studied separately by researchers from different communities, they share very similar mathematical nature. However, to the best of our knowledge, no attempt has been made to connect the twisted particle filter with the control-based importance sampling algorithms rigorously. In this paper, we build a bridge between these two problems under suitable settings for the discrete/continuous-time models (see Section 3 for more details). Moreover, based on this connection, we propose a novel algorithm called “Twisted-Path Particle Filter” (TPPF), which is directly guided by a family of control-based importance sampling algorithms, as well as parts of their theoretical foundations including the classical Donsker-Varadhan variational principle [4, 12, 30]. The proposed TPPF algorithm is expected to be more versatile, less problem-dependent, and behave better in high dimensions (see detailed discussions at the beginning of Section 4). Some numerical examples are given in Section 5 to validate the TPPF and compare it with existing approaches.

1.1 Related works

Twisted particle filters (TPF). The idea of twisting the model in the discrete-time setting is well established. Various twisted particle filter algorithms have been proposed and studied by researchers from different areas of computational statistics or machine learning. In [52], the authors proposed the so-called “fully-adapted auxiliary particle filter” (FA-APF), where the “look-ahead” strategy was applied to twist the model, and they chose $g_k(\cdot)$ as the twisting function at each discrete time k . In [26], the authors proposed the “iterated auxiliary particle filter” (iAPF) algorithm, where they made use of the recursive relation of the optimal twisting function (see details in (2.11) below), and learned the twisting function

iteratively using Galerkin approximation with Gaussian basis functions. Similar approaches were adopted in [33], where the authors studied the problem from the view of discrete-time optimal control, and made some improvements to the learning structure for better numerical stability. Note that this fixed-point iteration method for approximating the optimal twisting function in [26, 33] shares a similar idea with the temporal difference (TD) method [58, 17, 49] widely used in the reinforcement learning (RL) community. This fixed-point iteration structure for learning the twisting function has been applied and improved in some other results for twisted particle filters such as [3, 41], where [3] made use of the rejection sampling to generate samples from the twisted Markov chain, and [41] adopted suitable neural networks to parameterize the twisting function instead of the Galerkin approximation. Besides the TD-type methods, the authors of [5] proposed an “optimized auxiliary particle filter” (OAPF) algorithm, where they solve adaptively an convex optimization problem at each discrete time k to update the weights and positions of particles when simulating the discrete Markov chains.

Learning-based TPF algorithms. Most TPF algorithms above are based on optimization over a Galerkin function space. More recently, designed for more practical tasks like large language modeling (LLM) in the machine learning community, some other deep-learning-based structures for approximating the optimal twisting function have been proposed. These learning-based algorithms include the Contrastive Twist Learning (CLT) in [67], the Future Discriminators for Generation (FUDGE) in [65], the SI \mathcal{X} O method in [40], to name a few. Basically, in these frameworks, they parameterized the twisting function via a suitable neural network, chose the summation of some specially designed quantities along the time axis as the loss function (for instance, in [67], they selected the KL-divergence at each time k determined by the current twisting function), and trained the network to obtain a good approximation of the optimal twisting functions. See more discussion on the choice of loss functions in Section 4 below. Compared with Galerkin-based methods, such neural network approximations are expected to have better behavior in high dimensions.

Continuous-time importance sampling (IS) via stochastic optimal control. As mentioned above, this paper connects the (continuous-time) control-based importance sampling and the (discrete-time) particle filters. From the theoretical perspective, the control-based importance sampling algorithms are well-studied in the importance sampling community. Various (continuous-time) importance sampling algorithms have been proposed, such as [38, 24, 1]. We are in particular interested in importance sampling algorithms for the path-dependent target (1.2), and focus on a sequence of control-based ones due to the zero-variance property related to the solution of the stochastic optimal control problem (see for instance [1, 30] or Proposition 2.3 below). A large amount of control-based importance sampling algorithm admits the structure of the continuous-time policy gradient (PG) method [64] (also called the iterative diffusion optimization (IDO) in some other literature [54]), and the corresponding details will be discussed later in Section 4.1. There are various classical choices for the loss function in the PG iteration in the existing literature. In the “cross-entropy” algorithm [66, 32], the loss is chosen as KL-divergence between path measures $D_{\text{KL}}(P^{u^*} \| P^u)$, where P^u is the path measure induced by the controlled SDE adding a control u to the drift, and P^{u^*} is the path measure corresponding to the optimal control u^* . Note that different from some other statistical inference problems, under the current setting, $D_{\text{KL}}(P^{u^*} \| P^u)$ has explicit expression and is even quadratic after suitable parameterization for the control function u . Other choices of the loss functions include the relative entropy loss $D_{\text{KL}}(P^u \| P^{u^*})$ [30, 44, 53], the variance loss (or log-variance loss) $\text{Var}_{P^v}(\frac{dP^{u^*}}{dP^u})$ (or $\text{Var}_{P^v}(\log \frac{dP^{u^*}}{dP^u})$) for some suitable basis path measure P^v [54], etc. Some theoretical bounds for the KL-type losses above were established in [29]. Besides the PG-based algorithms, other related importance sampling methods include the well-known forward-backward stochastic differential equation (FBSDE) approaches [36, 20, 60], where one approximates the target value Z via the solution of some SDE with given terminal-time state and a forward filtration.

Learning-based IS algorithms Many of the conventional methods above may suffer from the curse of dimensionality. In order to solve the related stochastic optimal control problem discussed above, a wide range of learning-based algorithms are available in reinforcement learning for the continuous-time setting. In these frameworks, the learning objective is usually parameterized by neural networks, and over decades a variety of these algorithms have been proposed and studied, such as the classical (soft) policy gradient [59, 64], actor-critic with temporal difference learning [68, 49] or with deep backward SDE [28], soft Q-learning [27, 56], etc. Other improvements to these learning-based frameworks include adding entropy regularization to the optimal control problem [61], and combining the metadynamics algorithms when X_s in (1.2) is trapped in some metastable region [53].

1.2 Main contributions

To end the introduction, we summarize the novelty and main contribution of our work here.

- First, to our knowledge, this paper is the first to rigorously build a bridge between (discrete-time) twisted particle filters and (continuous-time) control-based importance sampling algorithms. This connection is of great significance because through it we can (1) explore the continuous limit of some twisted particle filter algorithm and have a better understanding of its behavior from a continuous-time perspective; (2) propose novel twisted particle filter algorithms based on continuous-time importance sampling algorithms, which are well-studied and proved to have their own advantages when applied to suitable models.
- Second, our proposed algorithm TPPF treats the KL divergence between path measures as a loss function, and learns the optimal twisting function by neural networks. This approach can overcome the curse of dimensionality in many models compared with other Galerkin-based approximations for the optimal twisting functions. Moreover, TPPF is more robust and has a wider range of applications, because the learning procedure of the twisting function is problem-independent, which is different from other popular Galerkin-based methods [33, 26, 3, 41].

The rest of the paper is organized as follows. In Section 2, we introduce the basic settings of both discrete and continuous time cases. We also discuss the importance sampling for both models via the twisting function or control variate, respectively. The existence and the zero-variance property of the optimal twisting function / optimal control are also discussed in Section 2. In Section 3, under suitable assumptions, we prove the convergence from the discrete-time model to the continuous-time model. Based on the connection built in Section 3, and motivated by existing algorithms for the continuous-time model, we proposed a novel particle filter algorithm called “Twisted-Path Particle Filter” (TPPF) in Section 4. Several numerical examples are given in Section 5 to compare TPPF with existing approaches. A brief conclusion and some possible future work are summarized in Section 6. In the appendix, we provide the proofs of some technical lemmas and propositions.

2 Importance sampling for discrete-time and continuous-time models

In this section, we introduce both discrete-time and continuous-time models. For each model, after presenting the basic structure and the expression for the quantity of interest mentioned in (1.1), (1.2) above, we introduce the basic idea of variance reduction via importance sampling: Applying Girsanov’s transform, we provide an unbiased estimate for the target quantity, and meanwhile the variance could be reduced if we choose a suitable change of measure. As introduced in Section 1, this change of measure is in practice achieved by twisting the Markov chain. The twisting procedure is realized by multiplying some suitable function to the original transition kernel in the discrete setting, or adding a control variate to the drift in the continuous setting. Afterwards, for both models, we present the expressions of the optimal twisting function (for discrete setting) / optimal control variate (for

continuous setting). The optimal twisting function and the optimal control share similar zero-variance properties, similar backward-time evolution equations, and similar Feynman-Kac representations.

2.1 Discrete-time model and optimal twisting

Let us begin with the discrete-time model. Fix a positive integer n . Given a (time-homogeneous) Markov transition kernel $\hat{P}(x, dy)$ in \mathbb{R}^d (for simplicity we assume the corresponding transition density exists and still denote it by $\hat{P}(\cdot, \cdot)$), a sequence of bounded, continuous, nonnegative function $\hat{g}_k(\cdot)$ ($0 \leq k \leq n$), and a (deterministic) initial point $x \in \mathbb{R}^d$, the general discrete-time model is determined by the triple $(\hat{P}(\cdot, \cdot), (\hat{g}_k(\cdot))_k, x)$: For the discrete Markov chain $\hat{X}_{0:n} (:= (\hat{X}_0, \hat{X}_1, \dots, \hat{X}_n))$ with transition kernel $\hat{P}(\cdot, \cdot)$ and initial state $\hat{X}_0 = x$, the statistical quantity of interest is given by

$$Z_{dis}(x) := \mathbb{E}_x \left[\prod_{k=0}^n \hat{g}_k(\hat{X}_k) \right], \quad (2.1)$$

where $\mathbb{E}_x[\cdot] := \mathbb{E}[\cdot \mid \hat{X}_0 = x]$.

Such a general model is often called the Feynman-Kac model [9, 3], and the quantity $Z_{dis}(x)$ corresponds to the terminal marginal measure in it. Note that throughout this paper, we consider the Markov chain with a homogeneous transition kernel and a fixed deterministic initial state. As common in the literature, such settings are only designed to simplify the arguments and notations, and all results in this paper can be easily extended to the Markov chains with inhomogeneous transition kernels and with random initial conditions.

Remark 2.1 (state space model). *A special case of the general model above is the Hidden Markov Model (a state space model with finite states), where the functions $\hat{g}_{0:n}(\cdot)$ are determined on the random observation values $y_{1:n}$ with an observation conditional density function $\hat{g}_{y|x}^k(\cdot \mid \hat{X}_k)$ at each time k :*

$$\hat{X}_i \sim \hat{P}(\hat{X}_{i-1}, \cdot), \quad \hat{Y}_i \sim \hat{g}_{y|x}^i(\cdot \mid \hat{X}_i), \quad 0 \leq i \leq n.$$

Then, given the observations $y_{0:n}$, the functions $\hat{g}_{0:n}(\cdot)$ are given by

$$\hat{g}_k(\cdot) := \hat{g}_{x|y}^k(\cdot \mid \hat{Y}_j = y_j, j \leq k).$$

Consequently, conditioning on the observations $y_{0:n}$, the distribution of $\hat{X}_{1:n}$ is proportional to

$$\hat{g}_0(x_0) \prod_{k=1}^n \hat{g}_k(x_k) \hat{P}(x_{k-1}, x_k) dx_{1:n},$$

and its normalizing constant is $Z_{dis}(x)$ defined in (2.1). Moreover, in order to compare with the time-continuous model driven by the Brownian model, later on we will consider the Gaussian transition (denoted by $\hat{P}^\eta(\cdot, \cdot)$) with a given drift function $b(\cdot)$ and time step η . Namely, the more special case where

$$\hat{P}^\eta(x, dy) := (4\pi\eta)^{-\frac{d}{2}} \exp\left(-\frac{1}{4\eta}|y - x - \eta b(x)|^2\right) dy. \quad (2.2)$$

Now, with the triple $(\hat{P}(\cdot, \cdot), (\hat{g}_k(\cdot))_k, x)$ of the discrete model, we aim to calculate $Z_{dis}(x)$. A standard approach is the particle filter method (also known as sequential Monte Carlo) [16, 13, 15, 14, 46], where the expectation in $Z_{dis}(x)$ is simulated via Monte Carlo. A classical particle filter algorithm is the following bootstrap particle filter (BPF) [25]:

Algorithm 1 Bootstrap particle filter (BPF)

Given $(\hat{P}(\cdot, \cdot), (\hat{g}_k(\cdot))_k, x)$ and particle number N . Set $\zeta_0^i = x$, $1 \leq i \leq N$.

For $k = 1, \dots, n$,

1. Calculate the particle weights

$$W_{k-1}^j = \frac{\hat{g}_{k-1}(\zeta_{k-1}^j)}{\sum_{\ell=1}^N \hat{g}_{k-1}(\zeta_{k-1}^\ell)}, \quad 1 \leq j \leq N. \quad (2.3)$$

2. Sample independently

$$\zeta_k^i \sim \sum_{j=1}^N W_{k-1}^j \hat{P}(\zeta_{k-1}^j, \cdot), \quad 1 \leq i \leq N. \quad (2.4)$$

Output: ζ_k^i ($k = 0, \dots, n$, $i = 1, \dots, N$), $Z_{dis}^N(x) := \prod_{k=0}^n \frac{1}{N} \sum_{i=1}^N \hat{g}_k(\zeta_k^i)$.

Note that for each k , in (2.4), particles are resampled according to the weights $W_{k-1}^{1:N}$ defined in (2.3). An effective way to implement (2.4) is the ancestor-prediction method (see for instance [26, 3]), namely, at k -th step,

1. Sample ancestors $A_{k-1}^i \sim \mathcal{C}(W_{k-1}^1, \dots, W_{k-1}^N)$, $1 \leq i \leq N$.

2. Sample predictions $\zeta_k^i \sim \hat{P}(\zeta_{k-1}^{A_{k-1}^i}, \cdot)$, $1 \leq i \leq N$.

Above, $\mathcal{C}(\cdot, \dots, \cdot)$ denotes the categorical distribution to sample the indexes. Moreover, the resampling step does not need to occur at each step, and one improvement is the κ -adapted resampling [39, 45, 11], where the resampling step only occurs when the effective sample size is smaller than κN for some fixed $\kappa \in (0, 1)$.

For any $w^{1:N}$ with $\sum_{i=1}^N w^i = 1$, the effective sample size $ESS(w^{1:N})$ is defined by

$$ESS(w^{1:N}) := 1 / \sum_{i=1}^N (w^i)^2,$$

and it is a good standard to evaluate a particle filter algorithm - higher ESS usually means better performance.

One of the shortcomings of BPF is the relatively high variance, especially when the dimension d or the length of the Markov chain n is large. The twisted particle filter was introduced [33, 26, 3, 63, 5, 67, 41, 40] to reduce the variance of $Z_{dis}(x)$ defined in (2.1) based on importance sampling. The general idea is to use the (discrete-time) change of measure, or equivalently, a sequence of twisting functions $\varphi(k, \cdot)$ ($1 \leq k \leq n$). Then, we consider the twisted model with the triple $(\hat{P}^\varphi(\cdot, \cdot), (\hat{g}_k^\varphi(\cdot))_k, x)$ defined by

$$\hat{P}_k^\varphi(x, dy) := \frac{\varphi(k, y)}{\hat{P}[\varphi](k, x)} \hat{P}(x, dy), \quad \hat{P}[\varphi](k, x) = \int \varphi(k, y') \hat{P}(x, dy') \quad 1 \leq k \leq n, \quad (2.5)$$

$$\hat{g}_k^\varphi(x) := \hat{g}_k(x) \ell_k^\varphi(x), \quad 0 \leq k \leq n, \quad (2.6)$$

with

$$\ell_0^\varphi(x) := \hat{P}[\varphi](1, x), \quad \ell_n^\varphi(x) := \frac{1}{\varphi(n, x)}, \quad \ell_k^\varphi(x) := \frac{\hat{P}[\varphi](k+1, x)}{\varphi(k, x)}, \quad 1 \leq k \leq n-1. \quad (2.7)$$

Then it is not difficult to check that the twisted model preserves the quantity (2.1). We conclude this property in the following proposition (see Appendix A for a detailed proof):

Proposition 2.1. Consider the twisted model defined in (2.5)–(2.7). Recall the quantity $Z_{dis}(x)$ defined in (2.1). Then

$$Z_{dis}(x) = \mathbb{E}_x \left[\prod_{k=0}^n \hat{g}_k^\varphi(\hat{X}_k^\varphi) \right], \quad (2.8)$$

where \hat{X}^φ is the twisted Markov chain with the (time-inhomogeneous) transition kernel $\hat{P}_k^\varphi(\cdot, \cdot)$, namely, $\hat{X}_k^\varphi \sim \hat{P}_k^\varphi(\hat{X}_{k-1}^\varphi, \cdot)$ ($1 \leq k \leq n$).

Remark 2.2 (discrete-time change of measure). Proposition 2.1 is in fact the Girsanov's transform in the discrete-time setting. Denote \hat{P} the law of the untwisted Markov chain $\hat{X}_{0:n}$ with the transition kernel $\hat{P}(\cdot, \cdot)$, and denote \hat{P}^φ the law of the twisted Markov chain $\hat{X}_{0:n}^\varphi$ with the transition kernel $\hat{P}^\varphi(\cdot, \cdot)$. Then, the Girsanov transform gives

$$Z_{dis}(x) = \mathbb{E}_x^{X \sim \hat{P}} \left[\prod_{k=0}^n \hat{g}_k(X_k) \right] = \mathbb{E}_x^{X \sim \hat{P}^\varphi} \left[\prod_{k=0}^n \hat{g}_k(X_k) \frac{d\hat{P}}{d\hat{P}^\varphi}(X) \right],$$

where the Radon-Nikodym derivative is given by

$$\frac{d\hat{P}}{d\hat{P}^\varphi}(X) = \prod_{k=0}^n \ell_k^\varphi(X_k) = \prod_{k=1}^n \frac{\hat{P}[\varphi](k, X_{k-1})}{\varphi(k, X_k)}.$$

With the twisted model (2.5) - (2.7) and Proposition 2.1, it is natural to consider the following twisted particle filter (TPF) method [33, 26, 3, 63, 5, 67, 41, 40], whose output $Z_{dis}^{N,\varphi}(x)$ defined below approximates our target quantity $Z_{dis}(x)$ due to law of large number (see for instance, Proposition 3 in [26], or Section 3.6 in [16]):

Algorithm 2 Twisted particle filter (TPF)

Given $\varphi(\cdot, \cdot)$, $(\hat{P}^\varphi(\cdot, \cdot), (\hat{g}_k^\varphi(\cdot))_k, x)$ and particle number N . Set $\zeta_0^i = x$, $1 \leq i \leq N$.

For $k = 1, \dots, n$,

1. Calculate the particle weights

$$W_{k-1}^j = \frac{\hat{g}_{k-1}^\varphi(\zeta_{k-1}^j)}{\sum_{\ell=1}^N \hat{g}_{k-1}^\varphi(\zeta_{k-1}^\ell)}, \quad 1 \leq j \leq N. \quad (2.9)$$

2. Sample independently

$$\zeta_k^i \sim \sum_{j=1}^N W_{k-1}^j \hat{P}(\zeta_{k-1}^j, \cdot), \quad 1 \leq i \leq N. \quad (2.10)$$

Output: ζ_k^i ($k = 0, \dots, n$, $i = 1, \dots, N$), $Z_{dis}^{N,\varphi}(x) := \prod_{k=0}^n \frac{1}{N} \sum_{i=1}^N \hat{g}_k^\varphi(\zeta_k^i)$.

Now since the φ -twisted model (recall its definition (2.5)–(2.7)) obtains an unbiased estimation for the quantity $Z_{dis}(x)$ by Proposition 2.1, it is natural to ask the following question: How do we choose φ to minimize the variance. In fact, it is possible to choose an optimal twisting function sequence $\varphi^*(k, \cdot)$ ($1 \leq k \leq n$), under which the random variable $\prod_{k=0}^n \hat{g}_k^{\varphi^*}(\hat{X}_k^{\varphi^*})$ is an unbiased estimate of $Z_{dis}(x)$ with zero variance. Optimal twisting functions have been widely studied in the literature [3, 33, 26, 5]. In particular, the optimal twisting function sequence $\varphi^*(k, \cdot)$ ($1 \leq k \leq n$) is defined recursively as follows:

$$\begin{aligned} \varphi^*(k, x) &= \hat{g}_k(x) \int \varphi^*(k+1, y) \hat{P}(x, dy), \quad 0 \leq k \leq n-1, \\ \varphi^*(n, x) &= \hat{g}_n(x). \end{aligned} \quad (2.11)$$

Then the optimal twisting function has the following useful properties:

Proposition 2.2. Consider the functions $\varphi^*(k, \cdot)$ ($1 \leq k \leq n$) defined by (2.11). Recall $\hat{X}_{0:n}$ is a Markov chain with transition density $\hat{P}(\cdot, \cdot)$. Then

1. $\varphi^*(k, \cdot)$ satisfies

$$\varphi^*(k, x) = \mathbb{E} \left[\prod_{i=k}^n \hat{g}_i(\hat{X}_i) \mid \hat{X}_k = x \right], \quad 0 \leq k \leq n, \quad x \in \mathbb{R}^d. \quad (2.12)$$

In particular, $Z_{dis}(x) = \varphi^*(0, x)$, $\forall x \in \mathbb{R}^d$.

2. (zero variance property) Consider the Markov chain $\hat{X}_{0:n}^{\varphi^*}$ with the initial state $\hat{X}_0^{\varphi^*} = x$ and the transition density

$$\hat{P}_k^{\varphi^*}(x, y) := \frac{\varphi^*(k, y)}{\int \varphi^*(k, y') \hat{P}(x, y') dy'} \hat{P}(x, y), \quad 1 \leq k \leq n, \quad (2.13)$$

Define

$$\hat{W}(\hat{X}^{\varphi^*}) := \hat{L}(\hat{X}^{\varphi^*}) \prod_{k=0}^n \hat{g}_k(\hat{X}_k^{\varphi^*}) \quad (2.14)$$

with $\hat{L}(\hat{X}^{\varphi^*}) := \prod_{k=0}^n \ell_k^*(\hat{X}_k^{\varphi^*})$ and

$$\begin{aligned} \ell_0^*(x) &:= \int \varphi^*(1, y) \hat{P}(x, dy), & \ell_n^*(x) &:= \frac{1}{\varphi^*(n, x)}, \\ \ell_k^*(x) &:= \frac{\int \varphi^*(k+1, y) \hat{P}(x, dy)}{\varphi^*(k, x)}, & 1 \leq k \leq n. \end{aligned} \quad (2.15)$$

Then, $\hat{W}(\hat{X}^{\varphi^*})$ is an unbiased estimate of $Z_{dis}(x)$ with zero variance. Namely,

$$\hat{W}(\hat{X}^{\varphi^*}) = \varphi^*(0, x) = Z_{dis}(x), \quad \forall x \in \mathbb{R}^d. \quad (2.16)$$

Proposition 2.2 has also been discussed in related literature such as [33, 26]. We provide a proof in Appendix A for completeness. Moreover, a direct corollary of the zero-variance property in Proposition 2.2 is that, with the optimal twisting function, after Monte Carlo approximation with N samples, the output $Z_{dis}^{N, \varphi^*}(x)$ of twisted particle filter (Algorithm 2) is a perfect approximation of the target $Z_{dis}(x)$. We refer to Appendix A for a detailed proof.

Corollary 2.1. Consider the optimal twisting function defined in (2.11). Then for any positive integer N and $x \in \mathbb{R}^d$,

$$Z_{dis}^{N, \varphi^*}(x) = Z_{dis}(x). \quad (2.17)$$

Note that although the φ^* -twisted particle filter provides a perfect approximation for our target $Z_{dis}(x)$, it is impossible to implement the twisted particle filter (Algorithm 2) associated with φ^* in practice. The reason is that we need the pointwise value of the twisting function so that $\hat{X}_{k+1}^{\varphi^*}$ can be sampled from the distribution proportional to $\varphi^*(k, \cdot) \hat{P}(\hat{X}_{k-1}^{\varphi^*}, \cdot)$. Therefore, it is crucial to find suitable approaches to approximate the optimal twisting functions $\varphi^*(k, \cdot)$ ($1 \leq k \leq n$) to lower the variance of the particle filter algorithm. Moreover, due to the law of large numbers [16, 26], the larger sample size N and the better approximation of φ^* would give a better approximation for $Z_{dis}(x)$ (i.e. smaller variance of the numerical output $Z_{dis}^{N, \varphi^*}(x)$).

In Section 4, we will propose a new method to approximate φ^* , guided by similar method for the continuous-time model described in the following subsection.

2.2 Continuous-time model and optimal control

In this subsection, we first define the time-continuous model and the target quantity. Then we introduce the control-based importance sampling method based on the Girsanov's theorem. In the end, we introduce the optimal control and its zero-variance property.

For a fixed function $b : \mathbb{R}^d \rightarrow \mathbb{R}^d$, we consider the following SDE

$$X_t = X_0 + \int_0^t b(X_s) ds + \sqrt{2} B_t, \quad X_0 = x \in \mathbb{R}^d. \quad (2.18)$$

where $(B_t)_{t \geq 0}$ is the Brownian motion in \mathbb{R}^d under the probability measure P . The dynamics is thus a time-homogeneous Markov process with transition density (or Green's function) $P_t(y|x)$ satisfying a Fokker-Planck equation

$$\partial_t P_t(y|x) = -\nabla_y \cdot (b(y) P_t(y|x)) + \Delta_y P_t(y|x), \quad P_0(y|x) = \delta_x(y), \quad (2.19)$$

where $\delta_x(\cdot)$ is the Dirac delta at x . Moreover, given functions $h(t, x)$, $g(x)$ and $T > 0$, the general continuous model is determined by $(P; h, g; x)$, and the corresponding statistical quantity of interest is

$$Z_{con}(x) = \mathbb{E}_x \left[e^{\int_0^T h(s, X_s) ds} g(X_T) \right], \quad (2.20)$$

Remark 2.3 (state space model). *Recall the example in Remark 2.1. Here, a corresponding special case is the latent SDE model, which is a state space model which has infinitely many states. In detail, the functions $h(t, x)$ and $g(x)$ are determined by the value of a random observation process Y_t conditional on X_t , i.e.*

$$X_t = x + \int_0^t b(X_s) ds + \sqrt{2} B_t, \quad Y_t \sim g_{y|x}^t(\cdot | X_s, s \leq t), \quad 0 \leq t \leq T. \quad (2.21)$$

Denote the conditional density function (which is the density of $\text{Law}(X_t | y_s, s \leq t)$) by

$$g_t(\cdot) := g_{x|y}^t(\cdot | y_s : s \leq t),$$

and let

$$h(t, x) = \log g_t(x), \quad g(x) = g_T(x), \quad 0 \leq t \leq T, \quad x \in \mathbb{R}^d.$$

Then the target quantity $Z_{con}(x)$ is

$$Z_{con}(x) = \mathbb{E}_x \left[e^{\int_0^T \log g_s(X_s) ds} g_T(X_T) \right],$$

which is comparable with the discrete target $Z_{dis}(x)$, since $Z_{dis}(x)$ has the similar expression

$$Z_{dis}(x) = \mathbb{E}_x \left[\prod_{k=0}^{n-1} \hat{g}_k(\hat{X}_k) \right] = \mathbb{E}_x \left[e^{\sum_{k=0}^{n-1} \log \hat{g}_k(\hat{X}_k)} \hat{g}_n(\hat{X}_n) \right].$$

We will prove the convergence from $Z_{dis}(x)$ to $Z_{con}(x)$ in Section 3 below for the discrete transition kernel of the form (3.1).

We will give a concrete example in Example 3.1 of Section 3, where the function $g_t(\cdot) = g_{x|y}^t(\cdot | y_s : s \leq t)$ has an explicit expression. The example satisfies all the conditions required by the convergence analysis in Section 3 below.

Now, considering the general continuous model determined by $(P; h, g; x)$, we aim to calculate the quantity $Z_{con}(x)$. Similar to the discrete model, we approximate it via Monte Carlo using N samples:

$$Z_{con}(x) \approx Z_{con}^N(x) := \frac{1}{N} \sum_{i=1}^N e^{\int_0^T \log h(s, X_s^i) ds} g(X_T^i),$$

where X^1, \dots, X^N are N independent realizations of the SDE (2.18).

Next, we aim to reduce the variance of the random variable $Z_{con}^N(x)$. In fact,

$$\text{Var}(Z_{con}^N(x)) = \frac{1}{N} \text{Var}(e^{\int_0^T \log h(s, X_s) ds} g(X_T)).$$

Therefore, we aim to reduce the variance of the random variable $e^{\int_0^T \log h(s, X_s) ds} g(X_T)$ for X satisfying (2.18). Here, we also consider variance reduction via importance sampling, which is based on a change of measure, as discussed in the discrete case. In detail, the change of measure is constructed by adding a control variate u to the drift and considering the following controlled SDE:

$$X_t^u = X_0^u + \int_0^t (b(X_s^u) + \sqrt{2}u(s, X_s^u)) ds + \sqrt{2}W_t, \quad X_0^u = x \in \mathbb{R}^d. \quad (2.22)$$

Then, denoting the path measures $\mathcal{P} := \text{Law}(X_{[0,T]})$ (X solving (2.18)) and $\mathcal{P}^u := \text{Law}(X_{[0,T]}^u)$ (X^u solving (2.22)), the change of measure gives

$$\begin{aligned} Z_{con}(x) &= \mathbb{E}_x^{X \sim \mathcal{P}} \left[e^{\int_0^T \log h(s, X_s) ds} g(X_T) \right] \\ &= \mathbb{E}_x^{X \sim \mathcal{P}^u} \left[e^{\int_0^T \log h(s, X_s) ds} g(X_T) \frac{d\mathcal{P}}{d\mathcal{P}^u}(X) \right] = \mathbb{E}_x \left[e^{\int_0^T \log h(s, X_s^u) ds} g(X_T^u) \frac{d\mathcal{P}}{d\mathcal{P}^u}(X^u) \right], \end{aligned}$$

where the Radon-Nikodym derivative has the following expression due to Girsanov's theorem:

$$\frac{d\mathcal{P}}{d\mathcal{P}^u}(X^u) = \exp \left(- \int_0^T u(s, X_s^u) \cdot dB_s - \frac{1}{2} \int_0^T |u(s, X_s^u)|^2 ds \right).$$

Consequently, the following Monte-Carlo approximation is an unbiased estimate of the target $Z_{con}(x)$:

$$Z_{con}^{N,u}(x) := \frac{1}{N} \sum_{i=1}^N e^{\int_0^T \log h(s, X_s^{i,u}) ds} g(X_T^{i,u}) \frac{d\mathcal{P}}{d\mathcal{P}^u}(X^{i,u}),$$

where $X^{1,u}, \dots, X^{N,u}$ are N independent realizations of the controlled SDE (2.22).

Our goal is to minimize the variance of $e^{\int_0^T \log h(s, X_s^u) ds} g(X_T^u) \frac{d\mathcal{P}}{d\mathcal{P}^u}(X^u)$ for u belonging to some suitable admissible set. Luckily, we can find an optimal control (similar to the discrete case) satisfying a zero-variance property, and then we only need to find suitable approaches to approximate the optimal control. In fact, the optimal control u^* is given by

$$u^*(t, x) = \sqrt{2} \partial_x \log v^*(t, x),$$

where $v^*(t, x)$ satisfies the following backward Kolmogorov (parabolic) equation:

$$\begin{aligned} -\partial_t v^*(t, x) &= b(x) \cdot \nabla_x v^*(t, x) + \Delta_x v^*(t, x) + h(t, x) v^*(t, x), \quad 0 \leq t \leq T, \\ v^*(T, x) &= g(x). \end{aligned} \quad (2.23)$$

Moreover, the following Feynman-Kac representation and zero-variance property hold:

Proposition 2.3. *Fix $T > 0$ and $x \in \mathbb{R}^d$. Given functions $h : \mathbb{R}_+ \times \mathbb{R}^d \rightarrow \mathbb{R}$, $g : \mathbb{R}^d \rightarrow \mathbb{R}$, $b : \mathbb{R}^d \rightarrow \mathbb{R}^d$,*

1. (Feynman-Kac representation) *The solution to the PDE (2.23) has the following representation:*

$$v^*(t, x) = \mathbb{E} \left[e^{\int_t^T h(s, X_s) ds} g(X_T) \mid X_t = x \right], \quad 0 \leq t \leq T, \quad x \in \mathbb{R}^d, \quad (2.24)$$

where the process X_t solves the SDE (2.18). In particular, $Z_{con}(x) = v^*(0, x)$, $\forall x \in \mathbb{R}^d$.

2. (zero-variance property) Let P be the probability measure such that under which $(B_t)_{t \geq 0}$ is a Brownian motion in \mathbb{R}^d . Then there exists a probability measure P^* such that under P^* , the law of the controlled process with control $u^* = \sqrt{2} \partial_x \log v^*$

$$X_t^{u^*} = X_0^{u^*} + \int_0^t \left(b(X_s^{u^*}) + 2 \partial_x \log v^*(s, X_s^{u^*}) \right) ds + \sqrt{2} B_t, \quad X_0^{u^*} = x$$

is the same of the law of X_t under P (recall that X_t satisfies (2.18)). Moreover, define

$$L(T) := \exp \left(- \int_0^T \partial_x \log v^*(s, X_s^{u^*}) dB_s - \frac{1}{2} \int_0^T \left| \partial_x \log v^*(s, X_s^{u^*}) \right|^2 ds \right),$$

and

$$W := e^{\int_0^T h(s, X_s^{u^*}) ds} g(X_T^{u^*}) L(T).$$

We have

$$W = v^*(0, x) = Z_{con}(x) \quad P^* - a.s. \quad (2.25)$$

3 Convergence analysis: From discrete-time to continuous-time models

In Section 2 above, we have introduced the importance sampling for discrete/continuous-time models. Now we aim to build a bridge between the discrete-time results and the continuous-time results. The benefit of such connection is evident: Given an existing importance sampling algorithm in the continuous-time setting (approximating the optimal control), we can design the corresponding particle filter algorithm (approximating the optimal twisting function) in the discrete-time setting. Obviously, this also works in the reverse direction. Indeed, we will provide a concrete example for algorithm design in Section 4.

Now, in order to study the connection between the discrete and continuous models, we need the following restriction for their transition kernels P , \hat{P} and the functions determining the targets $Z_{con}(x)$, $Z_{dis}(x)$, so that we can establish the convergence results rigorously below. In detail, fix the function $b : \mathbb{R}^d \rightarrow \mathbb{R}^d$, time step $\eta > 0$, and $T := n\eta$. We consider the Gaussian transition kernel for the discrete model:

$$\hat{P}^\eta(x, dy) := (4\pi\eta)^{-\frac{d}{2}} \exp \left(-\frac{1}{4\eta} |y - x - \eta b(x)|^2 \right) dy. \quad (3.1)$$

Recall that the transition kernel for the continuous model P_t is associated with the SDE (2.18) with drift $b(\cdot)$ and volatility $\sqrt{2}$, and it satisfies the Fokker-Planck equation (2.19). Clearly, \hat{P}^η is the one-step transition kernel of the corresponding Euler-Maruyama scheme. Moreover, for convergence analysis in this section, we consider the discrete model determined by $(\hat{P}^\eta; \hat{g}_{0:n}(\cdot); x)$ and the continuous model determined by $(P_t; \log g(\cdot, \cdot), g_T(\cdot); x)$. Correspondingly, the statistical quantities of interest are respectively

$$Z_{dis}(x) := \mathbb{E}_x \left[\prod_{k=0}^{n-1} \hat{g}_k(\hat{X}_k) \hat{g}_n(\hat{X}_n) \right] = \mathbb{E}_x \left[\exp \left(\sum_{k=0}^{n-1} \int_{k\eta}^{(k+1)\eta} \log \left(\hat{g}_k(\hat{X}_k) \right)^{\eta^{-1}} ds \right) \hat{g}_n(\hat{X}_n) \right], \quad (3.2)$$

and

$$Z_{con}(x) = \mathbb{E}_x \left[\exp \left(\int_0^T \log g(s, X_s) ds \right) g_T(X_T) \right]. \quad (3.3)$$

In what follows, under suitable assumptions for the functions $b(\cdot)$, $\hat{g}_k(\cdot)$, $g(\cdot, \cdot)$ and $g_T(\cdot)$, we will consider the convergence from discrete-time model to the continuous-time model. In detail, we will show that at the time step $\eta \rightarrow 0$, \hat{P}^η converges to P_t , and $Z_{dis}(x)$ converges to $Z_{con}(x)$.

We need the following assumptions to ensure convergence:

Assumption 3.1. We assume the following conditions for $b : \mathbb{R}^d \rightarrow \mathbb{R}^d$, $\hat{g}_k : \mathbb{R}^d \rightarrow \mathbb{R}$ ($0 \leq k \leq n$), $g : \mathbb{R}_+ \times \mathbb{R}^d \rightarrow \mathbb{R}$ and $g_T : \mathbb{R}^d \rightarrow \mathbb{R}$:

- (a) $b(\cdot)$ is L_b -Lipschitz (i.e. $|b(x) - b(y)| \leq L_b|x - y|$, $\forall x, y \in \mathbb{R}^d$), and $\sup_{0 \leq i \leq n} \mathbb{E}|\hat{X}_{i\eta}|^2 < \infty$ uniform in η .
- (b) $\hat{g}_n(x) \rightarrow g_T(x)$, $\eta^{-1} \log \hat{g}_k(x) \rightarrow \log g(k\eta, x)$ uniformly in x and k ($0 \leq k \leq n - 1$) as $\eta \rightarrow 0$.
- (c) $\log g(t, x)$ is continuous in $t \in [0, T]$ uniform in x . $\eta^{-1} \log \hat{g}_{k\eta}(x)$ is Lipschitz in x uniformly for all k ($0 \leq k \leq n - 1$) and $\eta > 0$.
- (d) $\hat{g}_n(\cdot)$ is bounded. For any $t \in [0, T]$, the functional $X_{[t, T]} \mapsto e^{\int_t^T \log g(\tau, X_\tau) d\tau}$ is continuous and bounded.

Above, condition (a) is used to ensure the existence and uniqueness of the strong solution for (2.18) and the convergence of transition kernel in Proposition 3.1 below. Other conditions are required for the convergence of $Z_{dis}(x)$ to $Z_{con}(x)$ in Proposition 3.2 below. Also, we will give a concrete example in Example 3.1 below which satisfies all the conditions in Assumption 3.1.

We also remark here that the upper bound for the second moment $\sup_{0 \leq i \leq n} \mathbb{E}|\hat{X}_{i\eta}|^2$ can be proved if one assumes: (1) L_b -Lipschitz condition for $b(\cdot)$; (2) the following confining condition for $b(\cdot)$:

$$x \cdot b(x) \leq -C_1|x|^2 + C_2, \quad \forall x \in \mathbb{R}^d,$$

where C_1, C_2 are two positive constants. Moreover, under such assumptions, the upper bound $\sup_{0 \leq i \leq n} \mathbb{E}|\hat{X}_{i\eta}|^2$ can be shown to be independent of the time T (recall that $T = n\eta$).

In the following proposition, we establish the convergence of transition kernels in terms of the KL-divergence or the total variation (TV) distance. Note that for two probability measures μ, ν on \mathbb{R}^d , the KL-divergence and TV distance are given by

$$D_{\text{KL}}(\mu \parallel \nu) := \begin{cases} \int_{\mathbb{R}^d} \log \frac{d\mu}{d\nu} \mu(dx), & \mu \ll \nu, \\ +\infty, & \text{otherwise.} \end{cases} \quad (3.4)$$

$$\text{TV}(\mu, \nu) := \sup_{A \in \mathcal{B}(\mathbb{R}^d)} |\mu(A) - \nu(A)|. \quad (3.5)$$

Proposition 3.1. Consider the Markov transition kernels \hat{P}^η and $P_\eta (= P_{t=\eta})$ defined in (3.1), (2.19), respectively. Suppose that the condition (a) in Assumption 3.1 holds. Then for any $x \in \mathbb{R}^d$, as $\eta \rightarrow 0$, $\hat{P}^\eta(x, \cdot) \rightarrow P_\eta(x, \cdot)$ in terms of KL-divergence or TV distance. In detail, for $\eta < 1$, there exists a positive constant C independent of η and d such that

$$D_{\text{KL}}(\hat{P}^\eta(x, \cdot) \parallel P_\eta(x, \cdot)) \leq Cd\eta^2 \rightarrow 0 \quad \text{as } \eta \rightarrow 0, \quad (3.6)$$

and

$$\text{TV}(\hat{P}^\eta(x, \cdot), P_\eta(x, \cdot)) \leq C\sqrt{d}\eta \rightarrow 0 \quad \text{as } \eta \rightarrow 0. \quad (3.7)$$

Note that the Proposition considers the local truncation error of the Euler-Maruyama scheme in terms of TV distance and KL divergence, consistent with the existing results [8]: consider the solution X_t ($t \geq 0$) to the continuous-time SDE (2.18) and its Euler-Maruyama discretization $\hat{X}_{n\eta}$ ($n \in \mathbb{N}_+$) with time step η , for any time interval length T such that η divides T , one can show that

$$D_{\text{KL}}(\text{Law}(\hat{X}_T) \parallel \text{Law}(X_T)) \lesssim T\eta.$$

This then reduces to (3.6) when $T = \eta$. Moreover, recent literature (for instance, [48, 43]) has shown that, if one assumes stronger smoothness conditions for the drift $b(\cdot)$, it is possible to improve the upper bound for the time-discretization error in terms of the KL-divergence from $O(T\eta)$ to $O(T\eta^2)$. Consequently, the rate in (3.6) is $O(\eta^3)$. The same arguments also hold for TV distance via Pinsker's inequality.

The next Proposition guarantees that under the settings of Assumption 3.1, the target $Z_{dis}(x)$ converges to $Z_{con}(x)$ as $\eta \rightarrow 0$.

Proposition 3.2. For $x \in \mathbb{R}^d$, recall the definitions of $Z_{dis}(x)$, $Z_{con}(x)$ in (3.2), (3.3), respectively. Then under Assumption 3.1,

$$Z_{dis}(x) \rightarrow Z_{con}(x) \quad (3.8)$$

pointwisely as $\eta \rightarrow 0$.

Remark 3.1 (explicit convergence rate). Under current assumptions, one cannot obtain an explicit convergence rate due to conditions (b) and (c) in Assumption 3.1. However, if we use a stronger version Assumptions 3.1, it is possible to obtain an explicit rate. In fact, if we replace conditions (b) and (c) in Assumption 3.1 by the following stronger quantitative version

$$(b') \quad g_T(\cdot) \text{ is bounded. } |\hat{g}_n(x) - g_T(x)| \leq C_1 \eta^{\alpha_1}, \quad |\eta^{-1} \log \hat{g}_{k\eta}(x) - \log g_{k\eta}(x)| \leq C_2 \eta^{\alpha_2}, \\ 0 \leq k \leq n-1, \text{ where } C_1, C_2, \alpha_1, \alpha_2 \text{ are positive constants independent of } x, k.$$

$$(c') \quad \log g_s(x) \text{ is } \alpha_3\text{-H\"older continuous in } t \in [0, T] \text{ uniform in } x. \quad \eta^{-1} \log \hat{g}_{k\eta}(x) \text{ is Lipschitz in } x \text{ uniformly for all } k.$$

then, following exactly the same derivation, one can easily obtain for small η ,

$$|Z_{dis}(x) - Z_{con}(x)| \leq \eta^\alpha, \quad (3.9)$$

where $\alpha := \min(\frac{1}{2}, \alpha_1, \alpha_2, \alpha_3)$.

We end this section by giving a concrete example satisfying all the conditions in Assumption 3.1. In particular, it satisfies the time-continuity condition of $\log g(t, x)$, which might not be very direct at first glance.

Example 3.1 (an example satisfying time-continuity and other assumptions). Note that one important assumption is that the function $\log g(t, x)$ is time-continuous. Recall the state space models in Remark 2.1 and Remark 2.3. In such model, if the observation Y_t at time t only depends on the value of X_t (for instance, $Y_t \sim N(X_t, \Sigma)$ with Σ being a constant covariance matrix), then the time-continuity for the function $g_{x|y}^t$ would not hold, since the observation process Y itself is not continuous in time due to the randomness. However, we remark in the following that by considering time-dependency for $g_{y|x}^t$ (recall its definition in (2.21)), we can indeed find such time-continuous $\log g(t, x)$

In fact, we consider the following continuous-time state space model:

$$X_t = x + \int_0^t b(X_s) ds + \sqrt{2} B_t, \quad Y_t = X_t + \tilde{B}_{t+t_0}, \quad 0 \leq t \leq T \quad (3.10)$$

for two independent Brownian motions $(B_t)_{t \geq 0}$, $(\tilde{B}_t)_{t \geq 0}$. Here we introduce the positive constant t_0 only to avoid a potential singularity of $1/t$ at $t = 0$: As will be discussed below, the convergence would require the time continuity of $-\frac{|x-y_t|^2}{2(t+t_0)}$ in the closed interval $[0, T]$, thus the choice of some $t_0 > 0$.

Correspondingly, for the discrete model, for $0 \leq k \leq n$, we define \hat{Y}_k by

$$\hat{X}_{k+1} = \hat{X}_k + \eta b(\hat{X}_k) + \sqrt{2}(B_{(k+1)\eta} - B_{k\eta}), \quad \hat{Y}_k = \hat{X}_k + \tilde{B}_{k\eta+t_0}, \quad 0 \leq k \leq n. \quad (3.11)$$

Now suppose that we have been given observation y_t ($0 \leq t \leq T$) and \hat{y}_k ($0 \leq k \leq n$) (note that by our construction above, the observed process y_t of the continuous model is time-continuous). Clearly, the expressions for $g(t, x)$ and $\hat{g}_k(x)$ are explicit and are of the Gaussian form. Therefore in this case, we are able to convert the conditions in Assumption 3.1 for g and \hat{g} to assumptions for y and \hat{y} . Basically, defining $\mathcal{N}(\cdot; \mu, \Sigma)$ to be the density of d -dimension Gaussian distribution with mean μ and covariance Σ , we need the followings:

- $\mathcal{N}(x; \hat{y}_n, T + t_0) \rightarrow \mathcal{N}(x; y_n, T + t_0)$, $|x - \hat{y}_k|^2 \rightarrow |x - y_k|^2$ uniformly in x , k as $\eta \rightarrow 0$.
- For any $t \in [0, T]$, the functional $X_{[t, T]} \mapsto e^{\int_t^T -\frac{|X_\tau - y_\tau|^2}{2(\tau+t_0)} d\tau}$ is bounded.

- $-\frac{|x-y_t|^2}{2(t+t_0)}$ is continuous in $t \in [0, T]$ uniform in x . $-\frac{|x-\hat{y}_k|^2}{2(k\eta+t_0)}$ is Lipschitz in x uniformly for all k .

It is then easy to see that these conditions generally require (1) time-continuity for the observation y_t , (2) the observation for the two models $y_{k\eta}$, \hat{y}_k are very close. Clearly, since \hat{X} in (3.11) is the Euler-Maruyama discretization of X in (3.10), the continuous observed processes y , \hat{y} stay close when the time step η is small.

Furthermore, once these requirements are met, by Proposition 3.2, as $\eta \rightarrow 0$, the rescaled target

$$\tilde{Z}_{dis}(x) := \mathbb{E}_x \left[\prod_{k=0}^{n-1} (\hat{g}_k(\hat{X}_k))^{\eta^{-1}} \hat{g}_n(\hat{X}_n) \right]$$

converges pointwise to

$$Z_{con}(x) = \mathbb{E}_x \left[\exp \left(\int_0^T \log g(s, X_s) ds \right) g_T(X_T) \right].$$

As a final remark in this section, the time-continuity of the observation (in particular, the form (3.11)) is only required when proving the convergence from the discrete model to the continuous model. This discrete-continuous bridge then allows us to construct new twisted particle filters motivated by existing continuous-time importance sampling algorithms (e.g., see Section 4). However, since we construct algorithms directly for the discrete setting, the new algorithm does not necessarily require such time-continuity condition of the observation. In fact, the proposed algorithms work for simple linear Gaussian models (see Section 5.2), whose observation can be defined by $Y_k \sim N(X_k, \Sigma)$ with Σ being a constant covariance matrix.

4 Twisted-Path Particle Filter (TPPF)

In this section, we give a concrete example of how to explore new twisted particle filters guided by continuous-time importance sampling algorithms. Recall that in Section 3, we have proved the convergence from the discrete model to the continuous model under suitable settings. As has been mentioned at the beginning of Section 3, this connection we found can guide us to explore novel particle filter algorithms based on existing methods in the continuous-time setting. In this section, motivated by mature algorithms from the continuous-time community, we propose a Twisted-Path Particle Filter (TPPF). In this new algorithm for the discrete-time model, we treat the KL-divergence between twisted path measures and the optimal path measures as the loss function, parameterize the twisting function via neural networks, and approximate the optimal twisting function via suitable optimization methods such as the stochastic gradient descent. We expect this proposed algorithm to have the following strengths:

1. By parameterizing the twisting function using neural networks, TPPF is expected to overcome the curse of dimensionality compared with algorithms based on Galerkin approximation.
2. Due to the universal approximation theorem of neural networks [7], TPPF is more versatile and less problem-dependent, while in some other existing algorithms, the twisting function is learnt within a problem-dependent function class.
3. Compared with some other frameworks for learning the twisting function (see [33, 26, 41] for instance), which are based on the backward recursive relation (2.11), our method has relatively stronger theoretical foundations (see Lemma 4.1, Proposition 4.2, Corollary 4.1 below).

In the rest of this section, we will first explain the motivation of TPPF by presenting one importance sampling algorithm mainly from a variational perspective. Then we will

formulate the details of the TPPF algorithm under the guidance of the existing continuous-time algorithm. Some theoretical results as well as implementation details will also be provided.

4.1 Motivation: importance sampling via variational characterization in continuous-time setting

In the continuous-time model, it has been relatively well-studied to find the optimal control variate from a variational perspective. In order to seek the optimal control variate with the zero variance property, instead of solving the PDE we derived in (2.19), people convert this to an optimal control problem from a variational perspective [30, 66, 53, 32]. We first give some basis on the so-called Donsker-Varadhan variational principle [4, 12, 30], which is independent of whether the model is time-continuous or time-discrete.

Lemma 4.1 (Donsker-Varadhan variational principle). *Given some function $W(\cdot) : \Omega \rightarrow \mathbb{R}$ and probability measure P on Ω , the following relation holds:*

$$-\log \mathbb{E}^{X \sim P} [\exp(-W(X))] = \inf_{Q \in \mathcal{P}(\Omega)} \{ \mathbb{E}^{X \sim Q} [W(X)] + \text{D}_{\text{KL}}(Q \| P) \}, \quad (4.1)$$

where the minimum is over all probability measures on Ω .

Take Ω to be the path space corresponding to the continuous-time model and choose $W(\cdot)$ to be the path integral for some stochastic process $(X_s)_{0 \leq s \leq T}$, as in [30, 66, 53, 32]

$$W(X) := - \int_0^T h(s, X_s) ds - \log g(X_T)$$

for some $h(\cdot, \cdot)$, $g(\cdot)$ defined in Section 2.2, the variational relation (4.1) becomes

$$\begin{aligned} & -\log \mathbb{E}^{X_{[0,T]} \sim P} \left[\exp \left(\int_0^T h(s, X_s) ds + \log g(X_T) \right) \right] \\ &= \inf_{Q \in \mathcal{P}(\Omega), Q \ll P} \mathbb{E}^{X_{[0,T]} \sim Q} \left[\int_0^T -h(s, X_s) ds - \log g(X_T) \right] + \text{D}_{\text{KL}}(Q \| P). \end{aligned}$$

In particular, if the path measure P above is the law of solution to some $X_{[0,T]}$ satisfies an SDE as introduced in Section 2.2

$$dX_t = b(X_t)dt + \sqrt{2}dW, \quad 0 \leq t \leq T, \quad X_0 = x, \quad (4.2)$$

then the probability Q above is characterized by the path measure of the controlled SDE after adding a control variate u to the drift. In detail, consider the controlled the SDE

$$dX_t^u = b(X_t^u)dt + \sqrt{2}u(t, X_t^u)dt + \sqrt{2}dW, \quad 0 \leq t \leq T, \quad X_0^u = x. \quad (4.3)$$

By Girsanov's theorem, the dual relation (4.1) becomes

$$\begin{aligned} & -\log \mathbb{E}_x \left[\exp \left(\int_0^T h_s(X_s) ds + \log g_T(X_T) \right) \right] \\ &= \inf_{u \in \mathcal{U}} \mathbb{E}_x \left[- \int_0^T h_s(X_s^u) ds + \frac{1}{2} \int_0^T |u_s(X_s^u)|^2 ds - \log g(X_T^u) \right], \end{aligned}$$

and under the setting of Section 2.2, the set of admissible controls \mathcal{U} is usually chosen to be as follows (see for instance Section 1 in [54])

$$\mathcal{U} = \{ u \in C^1(\mathbb{R}^d \times [0, T], \mathbb{R}^d) : u \text{ grows at most linearly in } x \}.$$

Denote

$$J(u) := \mathbb{E}_x \left[- \int_0^T h_s(X_s^u) ds + \frac{1}{2} \int_0^T |u_s(X_s^u)|^2 ds - \log g(X_T^u) \right].$$

It can be verified that the minimizer u^* of the functional $J(u)$ yields a zero-variance importance sampler in Proposition 2.3 for the continuous setting, namely,

$$\exp\left(\int_0^T h(s, X_s^{u^*}) ds + \log g(X_T^{u^*})\right) \frac{dP}{dP^{u^*}}(X^{u^*}) = Z_{con}(x), \quad P^{u^*} - a.s.,$$

where P^{u^*} is the path measure induced by the controlled process X^{u^*} in (4.3) associated with the optimal control u^* , and P is the path measure induced by the original process X in (4.2). Therefore, it is reasonable to find the optimal control variates by solving the following stochastic optimal problem:

$$\min_{u \in \mathcal{U}} J(u) = \mathbb{E}_x \left[- \int_0^T h_s(X_s^u) ds + \frac{1}{2} \int_0^T |u_s(X_s^u)|^2 ds - \log g(X_T^u) \right]. \quad (4.4)$$

In practice, one may parameterize $u(t, x)$ by $u = u(\theta; t, x)$ and iteratively solve the optimization problem. In details, given a suitable loss function $L(u) = L(F(X_{[0,T]}^u, u))$ (e.g., $L = J$) in each iteration, one implement the followings:

1. With the current control $u(t, x) = u(\theta; t, x)$ simulate N realizations of the controlled SDE $X_{[0,T]}^u$, and calculate the loss L and its derivative $\nabla_\theta L$ using the N realizations of $X_{[0,T]}^u$.
2. Update θ using $\nabla_\theta L$ via some suitable method, for instance, the stochastic gradient descent.

As mentioned in Section 1, such an iterative framework is exactly the continuous-time policy gradient (PG) method [64], and it is also called the iterative diffusion optimization (IDO) in some other literature [54]. As a remark, $J(u)$ of the form (4.4) offers a good choice of the loss L , which equals to $D_{\text{KL}}(P^u \| P^{u^*})$ up to a constant. Moreover, people also studied other forms of loss to approximate the optimal control u^* , for instance, in the so-called cross-entropy method [66, 32], people use the loss $D_{\text{KL}}(P^{u^*} \| P^u)$ instead. More discussion on the choice of loss function and detailed derivations would be given in the next subsection for the TPPF algorithm, where we also treat the KL-divergence between path measures as the loss function.

4.2 Approximating the optimal twisting function in discrete-time setting

Now we propose a novel framework to approximate the optimal twisting function φ^* defined in (2.11), guided by the existing method for training u^* in the continuous-time setting. Different from the iteration method proposed in [33, 26, 41] (which is similar with the temporal difference (TD) learning in the reinforcement learning community [58, 17, 49, 68]) based on the recursive formula in (2.11), our method learns the optimal twisting function in the whole path via a neural network. Hence, we name the proposed algorithm the ‘‘Twisted-Path Particle Filter’’ (TPPF). As discussed at the beginning of Section 4, we expect the proposed method TPPF to (1) perform better in high dimensions; (2) be more robust and have wider applications; (3) have relatively stronger theoretical foundations.

In what follows, we first derive a similar variational principle and some relations between different choices of loss induced by the twisting function in the discrete-time setting. After that we would give our detailed algorithms corresponds to possible choices of loss function. Some detailed formulas and implement details will also be discussed at the end of this section.

First, note that the Donsker-Varadhan variational principle can also be applied to the discrete-time model in Section 2.1. In fact, after a change of measure, we have

$$-\log Z_{dis}(x) = \inf_{\varphi} J(\varphi),$$

where $\varphi = (\varphi_1, \dots, \varphi_n)$, $\varphi_i(\cdot)$ ($1 \leq i \leq n$) are positive, continuous functions in \mathbb{R}^d , and as a direct result of the dual relation, by choosing $W(\hat{X}) = -\sum_{k=0}^n \log \hat{g}_k(\hat{X}_k)$ for some discrete Markov chain $(\hat{X}_k)_{k=0}^n$

$$J(\varphi) := \mathbb{E}_x \left[-\sum_{k=0}^n \log \hat{g}_k(\hat{X}_k) \right] + \text{D}_{\text{KL}}(P^\varphi \| P^1), \quad (4.5)$$

where P^φ is the path measure induced by the twisting function φ as in (2.11), and the P^1 is the original path measure (or equivalently, with twisting function being 1). More precisely, under P^φ , the Markov chain X^φ evolves under the twisted transition density

$$\hat{P}_k^\varphi(x_{k-1}, x_k) = \frac{\varphi(k, x_k) \hat{P}(x_{k-1}, x_k)}{\hat{P}[\varphi](k, x_{k-1})}, \quad 1 \leq k \leq n,$$

with the normalizing constant $\hat{P}[\varphi](k, x_{k-1})$ defined by

$$\hat{P}[\varphi](k, x_{k-1}) = \int \varphi(k, y) \hat{P}(x_{k-1}, y) dy,$$

and under P the Markov chain X evolves under the untwisted transition density $\hat{P}(x_{k-1}, x_k)$. Consequently, the twisted path measure associated with the twisting function φ has the following explicit expression:

$$P^\varphi(dx_{1:n}) = \prod_{k=1}^n \frac{\varphi(k, x_k) \hat{P}(x_{k-1}, x_k)}{\hat{P}[\varphi](k, x_{k-1})} dx_{1:n}. \quad (4.6)$$

Similarly as in the continuous-time setting, it can be verified that the optimal twisting function φ^* with zero-variance property (discussed in Proposition 2.2) is the minimizer of the functional $J(\varphi)$ above, and minimizing the functional $J(\varphi)$ is equivalent to minimizing the KL-divergence $\text{D}_{\text{KL}}(P^\varphi \| P^{\varphi^*})$. We summarize this result in the Proposition below:

Proposition 4.1. *Consider the functional $J(\varphi)$ defined in (4.5) and the optimal twisting function φ^* defined in (2.11). Then it holds*

$$J(\varphi) = J(\varphi^*) + \text{D}_{\text{KL}}(P^\varphi \| P^{\varphi^*}).$$

Moreover, one can derive the following explicit formula for $J(\varphi)$ and $\text{D}_{\text{KL}}(P^\varphi \| P^{\varphi^*})$:

$$J(\varphi) = \mathbb{E}_x \left[-\sum_{k=0}^n \log \hat{g}_k(\hat{X}_k^\varphi) + \sum_{k=1}^n \log \frac{\varphi(k, \hat{X}_k^\varphi)}{\hat{P}[\varphi](k, \hat{X}_{k-1}^\varphi)} \right]$$

and

$$\text{D}_{\text{KL}}(P^\varphi \| P^{\varphi^*}) = \mathbb{E}_x \left[-\sum_{k=0}^n \log \hat{g}_k(\hat{X}_k^\varphi) + \sum_{k=1}^n \log \frac{\varphi(k, \hat{X}_k^\varphi)}{\hat{P}[\varphi](k, \hat{X}_{k-1}^\varphi)} \right] + \log \varphi_0^*(x)$$

Remark 4.1. *After a change of measure, it is easy to see that $J(\varphi)$ or $\text{D}_{\text{KL}}(P^\varphi \| P^{\varphi^*})$ has an alternative expression:*

$$\begin{aligned} \text{D}_{\text{KL}}(P^\varphi \| P^{\varphi^*}) &= \mathbb{E}_x \left[\exp \left(\sum_{k=1}^n \log \frac{\varphi_k(X_k)}{\tilde{\varphi}_{k-1}(X_{k-1})} \right) \right. \\ &\quad \left. \left(-\sum_{k=0}^n \log g_k(X_k) + \sum_{k=1}^n \log \frac{\varphi_k(X_k)}{\tilde{\varphi}_{k-1}(X_{k-1})} \right) \right] + \log \varphi_0^*(x). \end{aligned} \quad (4.7)$$

This expression is in particular useful in the cases where sampling from the original transition $\hat{P}(x_{k-1}, x_k)$ is much easier than sampling from the twisted transition $\hat{P}_k^\varphi(x_{k-1}, x_k)$. For

instance, if φ is parameterized by some neural network, basic sampling methods like rejecting sampler (proposed in [3] for the twisted particle filter) would not be so efficient, suffering from low, unstable acceptance rate. Moreover, it is natural to doubt whether the Monte Carlo approximation for the loss (and its gradient) would deteriorate after a change of measure. So far we have got no theoretical guarantee for this, but empirically, the experiments show that (4.7) can approximate the loss well.

Guided by various variational-based methods in continuous-time setting (discussed in Section 4.1), we can also consider different loss functions other than $J(\varphi)$ or $D_{\text{KL}}(P^\varphi \| P^{\varphi^*})$. Before seeking blindly for other possible choices, let us first study the relationship between the relative variance and KL-divergence, since our final goal of approximating the optimal twisting function is just to reduce the variance. In fact, using a generalized Jensen's inequality, we are able to derive the following:

Proposition 4.2. *Given some function $W(\cdot) : \Omega \rightarrow \mathbb{R}$ and probability measures $\nu, \tilde{\nu}$ on Ω which are absolutely continuous with each other, define*

$$Z := \mathbb{E}^{X \sim \nu} [e^{-W(X)}] = \mathbb{E}^{\tilde{X} \sim \tilde{\nu}} \left[e^{-W(\tilde{X})} \frac{d\nu}{d\tilde{\nu}}(\tilde{X}) \right]$$

and the relative variance with respect to $\tilde{\nu}$ defined by

$$r(\tilde{\nu}) := \frac{\sqrt{\text{Var}_{\tilde{\nu}} \left(e^{-W} \frac{d\nu}{d\tilde{\nu}} \right)}}{Z} \quad (4.8)$$

Suppose there is an optimal probability measure ν^* with the zero-variance property

$$\frac{d\nu^*}{d\nu} = \frac{e^{-W}}{Z} \quad \nu - a.s.,$$

Then the following estimates hold:

1. $r^2(\tilde{\nu}) \geq e^{\text{D}_{\text{KL}}(\nu^* \| \tilde{\nu})} - 1$
2. If the constants $m := \inf_E \frac{\nu^*(E)}{\tilde{\nu}(E)}$, $M = \sup_E \frac{\nu^*(E)}{\tilde{\nu}(E)}$ exist, then

$$e^{m \text{D}_{\text{KL}}(\tilde{\nu} \| \nu^*) + \text{D}_{\text{KL}}(\nu^* \| \tilde{\nu})} - 1 \leq r^2(\tilde{\nu}) \leq e^{M \text{D}_{\text{KL}}(\tilde{\nu} \| \nu^*) + \text{D}_{\text{KL}}(\nu^* \| \tilde{\nu})} - 1$$

Consider the discrete-time model with $(\hat{P}(\cdot, \cdot); \hat{g}_{0:n}(\cdot); x)$, we have the following direct corollary of Proposition 4.2.

Corollary 4.1. *Take $\Omega = \mathbb{R}^n$, $W(\hat{X}) = -\sum_{k=0}^n \log \hat{g}_k(\hat{X}_k)$, $\nu = P^1$, $\tilde{\nu} = P^\varphi$, and $\nu^* = P^{\varphi^*}$ (recall the definition of P^φ in (4.6)) in Proposition 4.2. Then there exists $0 < m \leq M$ depending on φ, φ^* such that*

$$e^{m \text{D}_{\text{KL}}(P^\varphi \| P^{\varphi^*}) + \text{D}_{\text{KL}}(P^{\varphi^*} \| P^\varphi)} - 1 \leq r^2(\tilde{\nu}) \leq e^{M \text{D}_{\text{KL}}(P^\varphi \| P^{\varphi^*}) + \text{D}_{\text{KL}}(P^{\varphi^*} \| P^\varphi)} - 1.$$

Motivated by Proposition 4.2 and Corollary 4.1 above, it is then reasonable to consider the loss function of the form

$$a \text{D}_{\text{KL}}(P^\varphi \| P^{\varphi^*}) + \text{D}_{\text{KL}}(P^{\varphi^*} \| P^\varphi)$$

for some positive a . Moreover, when P^φ approximates the target P^{φ^*} well, m, M in Proposition 4.2 are approximately 1, so it is reasonable to choose $a = 1$, namely, treat

$$\text{D}_{\text{KL}}(P^\varphi \| P^{\varphi^*}) + \text{D}_{\text{KL}}(P^{\varphi^*} \| P^\varphi)$$

as a loss function for $\tilde{\nu}$. Of course with these bounds, it is also reasonable to consider the loss

$$\text{D}_{\text{KL}}(P^{\varphi^*} \| P^\varphi),$$

which corresponds to the loss in the well-studied cross-entropy method in the continuous-time settings [66] (and this is the reason why we denote it by L_{CE}). When implementing the TPPF algorithm, we need explicit expressions for the loss functions chosen above, so that we can calculate them via Monte Carlo approximation. In fact, denoting

$$L_{RE} := D_{\text{KL}}(P^\varphi \| P^{\varphi^*}), \quad L_{CE} := D_{\text{KL}}(P^{\varphi^*} \| P^\varphi), \quad L_{RECE} = L_{RE} + L_{CE}. \quad (4.9)$$

Simple calculations yield

$$\begin{aligned} L_{RE} &= \mathbb{E}_x \left[-\sum_{k=0}^n \log \hat{g}_k(\hat{X}_k^\varphi) + \sum_{k=1}^n \log \frac{\varphi(k, \hat{X}_k^\varphi)}{\hat{P}[\varphi](k, \hat{X}_{k-1}^\varphi)} \right] + \log \varphi^*(0, x) \\ &= \mathbb{E}_x \left[\exp \left(\sum_{k=1}^n \log \frac{\varphi(k, \hat{X}_k)}{\hat{P}[\varphi](k, \hat{X}_{k-1})} \right) \left(-\sum_{k=0}^n \log \hat{g}_k(\hat{X}_k) + \sum_{k=1}^n \log \frac{\varphi(k, \hat{X}_k)}{\hat{P}[\varphi](k, \hat{X}_{k-1})} \right) \right] \\ &\quad + \log \varphi^*(0, x), \end{aligned} \quad (4.10)$$

where we can use either the first line (via the twisted Markov chain \hat{X}^φ) or the second line (via untwisted Markov chain \hat{X}) in the training. See Section 5 for more details. Also, for L_{CE} , we have

$$\begin{aligned} L_{CE} &= \frac{1}{\varphi_0^*(x)} \mathbb{E}_x \left[\exp \left(\sum_{k=0}^n \log \hat{g}_k(\hat{X}_k) \right) \left(\sum_{k=1}^n \log \hat{g}_k(\hat{X}_k) - \log \varphi^*(0, x) \right) \right] (= \text{constant}) \\ &\quad - \frac{1}{\varphi_0^*(x)} \mathbb{E}_x \left[\exp \left(\sum_{k=0}^n \log \hat{g}_k(\hat{X}_k) \right) \left(\sum_{k=1}^n \log \frac{\varphi(k, \hat{X}_k)}{\hat{P}[\varphi](k, \hat{X}_{k-1})} \right) \right], \end{aligned} \quad (4.11)$$

Remark 4.2 (possible numerical instability of L_{CE}). *Note that the coefficient*

$$\exp \left(\sum_{k=0}^n \log \hat{g}_k(\hat{X}_k) \right) / \varphi_0^*(x)$$

in second line of (4.11) may bring numerical instability to L_{CE} -training. First, it is possible that in some extreme cases, we have no idea of the value of $\varphi^(0, x)$ (which is our target $Z_{\text{dis}}(x)$), and sometimes we can't even get a good approximation of it. Second, this coefficient above is determined by \hat{g}_k and the (random) position of \hat{X}_k , so it is numerically unstable especially when the length of the Markov Chain n is large. Moreover, this observation is also empirically true in some examples, see details in Section 5.*

Given the loss functions above, to approximate optimal twisting function φ^* in practice, it is remaining to parameterize φ and learn the parameters according to the loss functions. In our algorithm, we parameterize the twisting function by neural network $\varphi_k(x) = \varphi(\theta; k, x)$, where θ denotes all the parameters of the network, and k, x are the input. For numerical stability, it is better to treat $\log \varphi(\theta; k, x) = NN(\theta; k, x)$ as the output so that $\varphi_k(x) = \exp(NN(\theta; k, x))$. We refer to Section 5 for more details and give the structure of the proposed TPPF in Algorithm 3 below:

Remark 4.3 (computing the gradient). *As a final remark, recall that when implementing Algorithm 3, we need to calculate the gradient $\nabla_\theta L$ via Monte Carlo approximation. Note that when the loss function L is approximated via the untwisted Markov Chain \hat{X} , the gradient can be calculated via auto-differentiation. However, if the loss L is approximated via the twisted Markov Chain \hat{X}^φ (see the first line in (4.10)), the computation of $\nabla_\theta L$ is not that direct, since \hat{X}^φ depends on the parameter θ . Here, we provide the explicit formula for $\partial_{\theta_i} L_{RE}$, where L_{RE} is given in the first line of (4.10). In fact, we first write L_{RE} into the form of the second line in (4.10), where \hat{X} in it is independent of θ . Then, after a change of measure, we can write the gradient into the following:*

$$\partial_{\theta_i} L_{RE} = \mathbb{E}_x \left[\left(1 - \sum_{k=1}^n \log \hat{g}_k(\hat{X}_k^\varphi) + \sum_{k=1}^n \log \frac{\varphi(k, \hat{X}_k^\varphi)}{\hat{P}[\varphi](k, \hat{X}_{k-1}^\varphi)} \right) \left(\sum_{k=1}^n \log \frac{\partial_{\theta_i} \varphi(k, \hat{X}_k^\varphi)}{\hat{P}[\partial_{\theta_i} \varphi](k, \hat{X}_{k-1}^\varphi)} \right) \right]. \quad (4.12)$$

Algorithm 3 Twisted-Path Particle Filter (TPPF)

Given discrete-time model with $(\hat{P}(\cdot, \cdot), (\hat{g}_k(\cdot))_k, x)$. Parameterized the twisting function via neural network: $\log \varphi(\theta; k, x) = NN(\theta; k, x)$. Choose the loss function $L = L_{RE}$ or L_{CE} or L_{RECE} .

1. **Learn the twisting function.** At each iteration,

(1) Simulate N independent realizations of the twisted Markov chain $\hat{X}_{0:n}^\varphi$ with transition kernel \hat{P}^φ (untwisted Markov chain $\hat{X}_{0:n}$ with transition kernel \hat{P}).

(2) Calculate the loss L and its gradient $\nabla_\theta L$ according to (4.9) - (4.12) via Monte Carlo approximation using the N samples obtained in (1).

(3) Update the parameters θ using suitable optimization methods (for instance, $\theta \leftarrow \theta - \eta \nabla_\theta L$).

2. **Run the twisted particle filter** (Algorithm 2) using the learned twisting function $\varphi(\theta; k, x)$

For a further implementation detail, to obtain $\partial_{\theta_i} L_{RE}$ in (4.12), there is no need to calculate $\partial_{\theta_i} \varphi$. Instead, we can first calculate the value of

$$\mathbb{E}_x \left[\left(1 - \sum_{k=1}^n \log \hat{g}_k(\hat{X}_k^\varphi) + \sum_{k=1}^n \log \frac{\varphi(k, \hat{X}_k^\varphi)}{\hat{P}[\varphi](k, \hat{X}_{k-1}^\varphi)} \right) \left(\sum_{k=1}^n \log \frac{\varphi(k, \hat{X}_k^\varphi)}{\hat{P}[\varphi](k, \hat{X}_{k-1}^\varphi)} \right) \right].$$

using Monte Carlo approximation, and then “detach” the first term above so that it would contain no gradient information. Consequently, auto-differentiation via (one-time) back-propagation gives the desired value of the gradient in (4.12).

5 Numerical examples

In this section, we test the proposed TPPF algorithm with loss function L_{RE} , L_{CE} , or L_{RECE} on different models including the linear Gaussian model, the Lorenz-96 model, and the stochastic volatility model. We compare our algorithm with well-known competitors including the bootstrap particle filter (BPF) [25], the iterated auxiliary particle filter (iAPF) [26], and the fully-adapted auxiliary particle filter (FA-APF) [52]. In most examples, TPPF performs better than other algorithms.

5.1 Implementation details

Before the main numerical experiment, let us give some details on how to parameterize the twisting function φ , how to sample from the twisted Markov transition kernel \hat{P}^φ , and how to calculate the normalizing constant $\hat{P}[\varphi](k, x)$. In fact, in the following three experiments, We consider two ways of parameterization: the robust non-parametric way and the problem-dependent parametric way. In particular, for the linear Gaussian model, we use the problem-dependent implementation, while for the other two models we use the non-parametric implementation.

1. The non-parametric implementation. As discussed in Section 4, we approximate the twisting function by

$$\log \varphi_k(x) = NN(\theta; k, x),$$

where $NN(\theta; k, x)$ is a neural network with parameters θ and inputs k, x ($0 \leq k \leq n$, $x \in \mathbb{R}^d$). In our experiments, we set NN as DenseNet [34, 54] with two hidden layers. Moreover, we add a tanh activation to the final layer so that the output $NN(\theta; k, x)$ takes value in $(\epsilon, 1)$, where $\epsilon > 0$ is a hyperparameter.

This bounded restriction is designed for the following reject sampling step when sampling from the twisted kernel \hat{P}^φ . In fact, since we usually do not have much information of the current twisting function φ , so it is not easy to sample from the twisting kernel $\hat{P}_k^\varphi(x, \cdot) \sim$

$\varphi(k, \cdot) \hat{P}(x, \cdot)$. Under the robust implementation setting, we make use of the reject sampling recently proposed in [3]: Using X_k^φ and the untwisted transition kernel $\hat{P}(X_k^\varphi, \cdot)$, propose a new position X_{pro} , accept it with probability $\varphi(X_{pro})$. Repeat until first acceptance.

Moreover, in the non-parametric implementation setting, the normalizing constant is calculated via Monte Carlo approximation using \tilde{N} samples (following [3], we choose $\tilde{N} = 50$ in both Lorenz-96 and NGM-78 models):

$$\hat{P}[\varphi](k, x) := \int \varphi(k, y) \hat{P}(x, dy) \approx \frac{1}{\tilde{N}} \sum_{i=1}^{\tilde{N}} \varphi(k, U_i), \quad U_i \sim \hat{P}(x, \cdot) \quad i.i.d.$$

Also, to make the training faster, we use the untwisted process X instead of X^φ when calculating the loss and the gradient (i.e. for L_{RE} , the loss is computed via the first line in (4.10) and its gradient is computed using (4.12)).

2. The parametric implementation. In the linear Gaussian model, we can calculate the analytical solution of $Z_{dis}(x)$ using the Kalman filter [35]. Moreover, we can analytically calculate the optimal twisting function using the backward recursive relation (2.11), and clearly the optimal twisting function is also Gaussian. Therefore, with so much knowledge of the solution, it is reasonable to consider a problem-dependent way to parameterize the twisting function to make the learning more efficient. In more details, via a mean-variance estimation framework, we set

$$\mu_k = NN_1(\theta_1; k) \in \mathbb{R}^d, \quad \sigma_k^2 = NN_2(\theta_2; k) \in \mathbb{R}_+, \quad 0 \leq k \leq n.$$

And then set

$$\varphi(k, x) = C_k N(x; \mu_k, \sigma_k^2). \quad (5.1)$$

Note that the twisting function is invariant of the constant scaling, so we do not care about the constant that multiplies the Gaussian. This means there is no need to learn C_k in (5.1), and in our experiment we just consider $C_k = (2\pi\sigma_k^2)^{-\frac{d}{2}}$ so that $\varphi(k, x) = \exp(-|x - \mu_k|^2 / 2\sigma_k^2)$. Also, under such settings, we no longer need the reject sampling and the inner-loop Monte Carlo for calculating the normalizing constant, because everything can be calculated analytically. Consequently, compared with the robust way, the problem-dependent implementation is less time consuming and the neural network is easier to train.

Another important remark is about the relative fairness of the comparisons in the numerical experiments. We learn and run the particle filter using the same particle numbers. For the time complexity, we admit that as a training-based algorithm, our algorithm is more time-consuming, and in fact, there is not a completely fair comparison due to different non-optimal choice of network structures. In order to conduct a relatively fair comparison, we restrict the number of iterations for the training so that the total running time is comparable and similar to its competitors.

5.2 Linear Gaussian model

As a first example, we consider the linear Gaussian model, which is also the discretization of an OU process X_t with linear Gaussian observations $Y_k \sim N(\cdot; B_k X_k, \Sigma_{OB})$

$$X_{k+1} = X_k + \Delta t A X_k + \sqrt{\Delta t} N(0, \Sigma).$$

We choose $\Delta t = 0.01$, $T = 0.5$ (so the length of the discrete Markov Chain is $n = T/\Delta t = 50$), $B_k = I_d$, $A = -I_d$, $\sigma = I_d$, $\Sigma_{OB} = I_d$.

We consider the parametric implementation with configurations $d \in \{2, 5, 15, 20\}$. The boxplots in Figure 1 compare the TPPF (with L_{RE} , L_{CE} , or L_{CERE}) with competitors including BPF, iAPF and FA-APF using 1000 replicates. The red cross represents the mean and the red dash line represents the medium. We also report the empirical standard deviations in Table 1, and in Table 2 we report the average relative effective sample size

(ESS-r) defined by $ESS(W_{1:N}) = 1/(N \sum_i^N W_i^2)$ with $\sum_{i=1}^N W_i = 1$. Clearly, TPPF with L_{RE} and L_{RECE} can defeat BPF and FA-APF, especially when the dimension is high, and TPPF with L_{CE} suffers from the curse of dimensionality due to the numerical instability discussed in Remark 4.2. Moreover, the iAPF performs the best in this linear Gaussian model, because iAPF is learning the twisting function in a Gaussian function class, each time solving a standard restricted least square minimization problem. Therefore, our training-based method cannot perform as well as iAPF in this experiment. However, as we will see in the other experiments when the optimal twisting function is not in the Gaussian family, our algorithm performs better than iAPF.

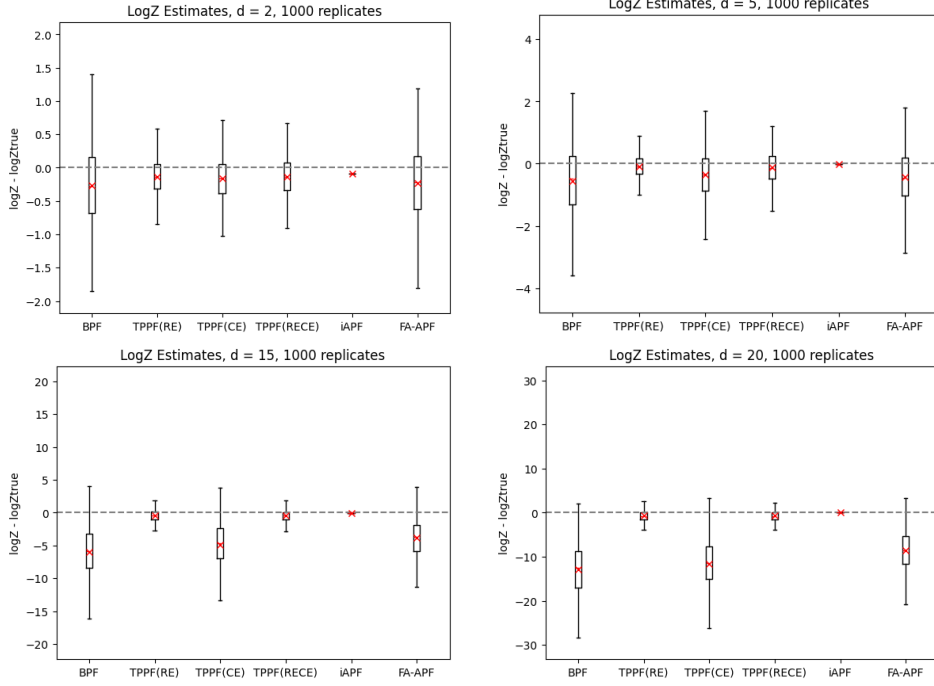


Figure 1: **Linear Gaussian model:** compare TPPF (trained with L_{RE} , L_{CE} , or L_{RECE}) and its competitors (BPF, iAPF and FA-APF). Boxplot for $\log Z$ using 1000 replicates, with configurations $d \in \{2, 5, 15, 20\}$. The red cross represents the mean and the red dash line represents the median.

	d=2	d=5	d=15	d=20
BPF	0.60	1.14	3.85	5.95
TPPF(RE)	0.27	0.38	0.87	1.23
TPPF(CE)	0.34	0.82	3.51	5.70
TPPF(RECE)	0.31	0.54	0.86	1.21
FA-APF	0.61	0.90	2.94	4.71
iAPF	6.11e-13	2.11e-14	1.13e-13	6.43e-14

Table 1: **Linear Gaussian model:** compare TPPF (trained with L_{RE} , L_{CE} , or L_{RECE}) and its competitors (BPF, iAPF and FA-APF). Empirical standard deviation of $\log Z$ with 1000 replicates for $d \in \{2, 5, 15, 20\}$.

	d=2	d=5	d=15	d=20
BPF	88.93%	73.93%	48.18%	41.38%
TPPF(RE)	91.42%	80.55%	55.87%	47.10%
TPPF(CE)	89.84%	74.64%	48.45%	41.59%
TPPF(RECE)	90.85%	79.11%	55.91%	47.09%
FA-APF	90.10%	76.29%	51.22%	44.24%
iAPF	100%	100%	100%	100%

Table 2: **Linear Gaussian model:** compare TPPF (trained with L_{RE} , L_{CE} , or L_{RECE}) and its competitors (BPF, iAPF and FA-APF). Averaged relative ESS with 1000 replicates for $d \in \{2, 5, 15, 20\}$.

5.3 NGM-78 model

In contrast to the linear nature of the last model, here we consider an (artificial) nonlinear model frequently used when testing the performance of particle filters [51, 25, 37, 62]. To our knowledge, this model was first used by Netto, Gimeno, and Mendes in 1978 [51], so here we name it NGM-78 model for simplicity. The NGM-78 model describes the following discrete-time Markov chain in \mathbb{R}^d :

$$X_n = a_0 X_{n-1} + a_1 \frac{X_{n-1}}{(1 + |X_{n-1}|^2)} + f(n) + v_n,$$

and the observations

$$Y_n = a_2 |Y_n|^2 + u_n,$$

where $v_n \sim N(0, \sigma_v^2 I_d)$ and $u_n \sim N(0, \sigma_u^2 I_d)$. In our experiments, we choose $a_0 = \frac{1}{2}$, $a_1 = 25$, $a_2 = \frac{1}{20}$, $f \equiv 0$, $\sigma_u^2 = 1$, $\sigma_v^2 = 0.01$, and $n = 0, 1, \dots, 50$. We test our TPPF algorithm on the NGM-78 model with the configuration $d \in \{1, 2, 5, 10, 15, 20\}$ and compare TPPF with its competitors. The empirical standard deviation of $\log Z$ is reported in Table 3. As we can see, in contrast to the linear Gaussian model, in the current nonlinear settings, the linear structure (twisted functions learned in some Gaussian function family) of iAPF leads to its relatively worse behavior. On the other hand, our TPPF algorithms behave better than iAPF partly due to the stronger expressive ability of neural networks. Moreover, in this model the term $\hat{P}[g](k, x)$ (recall the definition in (2.5)) used in FA-APF is calculated via Monte-Carlo approximation since there is not analytical solution for it. Consequently, we observe in Table 3 that although the FA-APF outperforms other algorithms when $d = 1$, it suffers from the curse of dimensionality and we cannot obtain reasonable estimates with the FA-APF in a feasible computational time.

	d=1	d=2	d=5	d=10	d=15	d=20
BPF	0.0243	0.118	0.156	0.163	0.252	0.295
TPPF(RE)	0.0184	0.0477	0.142	0.151	0.208	0.246
TPPF(CE)	0.0220	0.0657	0.220	0.266	0.183	0.273
TPPF(RECE)	0.0283	0.0483	0.140	0.160	0.187	0.280
FA-APF	0.00380	0.113	0.143	0.139	-	-
iAPF	0.0372	0.118	0.201	0.228	0.335	0.353

Table 3: **NGM-96 model:** compare TPPF (trained with L_{RE} , L_{CE} , or L_{RECE}) and its competitors (BPF, iAPF and FA-APF). Empirical standard deviation of $\log Z$ with 20 replicates for $d \in \{1, 2, 5, 10, 15, 20\}$. For $d \geq 15$, we cannot obtain reasonable estimates with the FA-APF in a feasible computational time.

5.4 Lorenz-96 model

The Lorenz-96 is a nonlinear model with partial observation [47, 33, 50]. The discrete model can be viewed as the Euler-Maruyama scheme of the following interacting particle system consisting of d particles in \mathbb{R}^1 :

$$dX^i = (-X^{i-1}X^{i-2} + X^{i-1}X^{i+1} - X^i + \alpha) dt + \sigma^2 dW^i, \quad 1 \leq i \leq d,$$

where $\alpha \in \mathbb{R}$, $\sigma^2 \in \mathbb{R}^+$, W^i ($1 \leq i \leq d$) are independent Brownian motions in \mathbb{R}^d , and the indices should be understood modulo d . The observation is through $Y_t \sim \mathcal{N}(\cdot; HX_t, \Sigma_{OB})$, where H is a diagonal matrix with $H_{ii} = 1$ ($1 \leq i \leq d-2$), $H_{ii} = 0$ ($d-1 \leq i \leq d$). Note that this model does not have an analytical solution. We use the non-parametric implementation in this example.

Choose $\alpha = 3.0$, $\Sigma_{OB} = I_d$, $\sigma = 1$. Consider $d \in \{3, 5, 10\}$. We report here the empirical standard deviations in Table 4 below:

	d=3	d=5	d=10
BPF	0.36	0.64	2.14
TPPF(RE)	0.26	0.43	1.23
TPPF(CE)	0.31	0.48	1.73
TPPF(RECE)	0.21	0.51	1.69
FA-APF	0.31	0.62	1.86
iAPF	0.29	0.48	1.81

Table 4: **Lorenz-96 model:** compare TPPF (trained with L_{RE} , L_{CE} , or L_{RECE}) and its competitors (BPF, iAPF and FA-APF). Empirical standard deviation of $\log Z$ with 20 replicates for $d \in \{3, 5, 10\}$.

To test the sensitivity of the proposed method, we fix $d = 3$, $\Sigma_{OB} = I_d$, $\sigma = 1$ and run the experiment for different α . See the results in Figure 2.

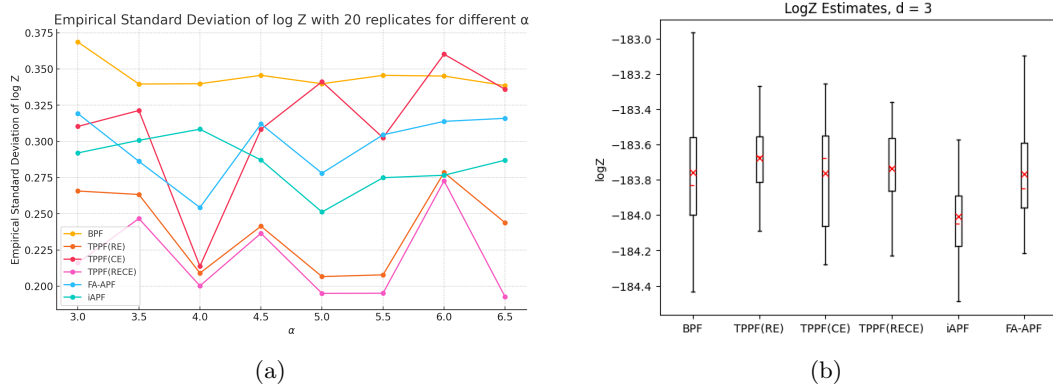


Figure 2: **Lorenz-96 model:** compare TPPF (trained with L_{RE} , L_{CE} , or L_{RECE}) and its competitors (BPF, iAPF and FA-APF). **(a):** Empirical standard deviation for different external force strength α under dimension $d = 3$, using 20 replicates. **(b):** Boxplot of $\log Z$ using 20 replicates for $d = 3$, $\alpha = 3.0$. The red cross represents the mean and the red dash line represents the median.

As we can see from Table 4 and Figure 2, the proposed TPPF algorithm (especially the ones using loss functions L_{RE} and L_{RECE}) behaves much better than BPF and FA-APF, and slightly better than iAPF. Moreover, we observe that for the current partial-observed nonlinear model, sometimes the result of iAPF is more biased (see (b) in Figure 2), despite its relatively low variance.

6 Conclusion

In this paper, we study the discrete-time twisted particle filters (TPF) from a continuous-time perspective. In detail, under suitable settings, we prove the convergence from discrete-time to continuous-time models. This then enables us to view existing control-based importance sampling algorithms as good guidance for constructing novel TPF algorithms in discrete-time settings. As a concrete example, we propose a novel TPF algorithm, Twisted-Path Particle Algorithm (TPPF), inspired by algorithms in continuous-time settings. In TPPF, we choose some specific KL-divergence between path measures as the loss function and learn the twisting function parameterized by a neural network. We also give some numerical examples to illustrate the capability of the proposed algorithm. Some possible future work may include: seeking other practical TPF algorithms guided by the continuous-time importance sampling algorithms, and understanding existing TPF algorithms rigorously by finding its continuous-time limit.

Acknowledgements

This work is supported in part by National Science Foundation via grant DMS-2309378. This work is done during Yuliang Wang's visit to Duke University. He thanks the Mathematics Department for their hospitality. The authors would thank PIERALBERTO GUARNIERO, ADAM M. JOHANSEN and ANTHONY LEE for help discussions on implementation details of iAPF method.

A Proofs of Section 2

A.1 Proof of Proposition 2.1

Proof. Recall the notation $\hat{P}[\varphi](k, x) = \int \varphi(k, y') \hat{P}(x, dy')$. Then by definition,

$$\begin{aligned} \mathbb{E}_x \left[\prod_{k=0}^n \hat{g}_k^\varphi(\hat{X}_k^\varphi) \right] &= \int \hat{g}_0^\varphi(x) \prod_{k=1}^n \hat{g}_k^\varphi(x_k) \hat{P}_k^\varphi(x_{k-1}, x_k) dx_{1:n} \\ &= \int \hat{g}_0(x) \left(\prod_{k=1}^n \hat{g}_k(x_k) \right) \left(\frac{\hat{P}[\varphi](1, x)}{\varphi(n, x_n)} \prod_{k=1}^{n-1} \frac{\hat{P}[\varphi](k+1, x_k)}{\varphi(k, x_k)} \prod_{k=1}^n \frac{\varphi(k, x_k)}{\hat{P}[\varphi](k, x_{k-1})} \hat{P}_k(x_{k-1}, x_k) \right) dx_{1:n} \\ &= \int \hat{g}_0(x) \prod_{k=1}^n \hat{g}_k(x_k) \hat{P}_k(x_{k-1}, x_k) dx_{1:n} = Z_{dis}(x). \end{aligned}$$

□

A.2 Proof Proposition 2.2

Proof. The proof is straightforward.

1. We first prove the first claim. Since $\varphi^*(n, x) = \hat{g}_n(x)$, direct calculation yields

$$\begin{aligned}
\varphi^*(n-1, x) &= \hat{g}_{n-1}(x) \int \hat{g}_n(y) \hat{P}(x, dy) = \mathbb{E} \left[\hat{g}_n(\hat{X}_n) \hat{g}_{n-1}(\hat{X}_{n-1}) \mid \hat{X}_{(n-1)} = x \right], \\
\varphi^*(n-2, x) &= \hat{g}_{n-2}(x) \int \mathbb{E} \left[\prod_{i=n-1}^n \hat{g}_i(\hat{X}_i) \mid \hat{X}_{n-1} = y \right] \hat{P}(x, dy) \\
&= \mathbb{E} \left[\prod_{i=n-2}^n \hat{g}_i(\hat{X}_i) \mid \hat{X}_{n-2} = x \right], \\
&\dots \\
\varphi^*(k, x) &= \hat{g}_k(x) \int \mathbb{E} \left[\prod_{i=k+1}^n \hat{g}_i(\hat{X}_i) \mid \hat{X}_{k+1} = y \right] \hat{P}(x, dy) \\
&= \mathbb{E} \left[\prod_{i=k}^n \hat{g}_i(\hat{X}_i) \mid \hat{X}_k = x \right], \\
&\dots \\
\varphi^*(0, x) &= \hat{g}_0(x) \int \mathbb{E} \left[\prod_{i=1}^n \hat{g}_i(\hat{X}_i) \mid \hat{X}_1 = y \right] \hat{P}(x, dy) \\
&= \mathbb{E} \left[\prod_{i=0}^n \hat{g}_i(\hat{X}_i) \mid \hat{X}_0 = x \right] = Z_{dis}(x).
\end{aligned}$$

2. Next, we prove the unbiased and zero-variance property of \hat{W} . The unbiased property is a direct result of Proposition 2.1 and Remark 2.2, and is valid for any twisting function sequence $\varphi(k, \cdot)$ ($1 \leq k \leq n$). To prove the zero variance property, we observe that under the probability measure P^* ,

$$\hat{W} = \prod_{k=0}^n \ell_k^*(\hat{X}_k) \prod_{k=0}^n \hat{g}_k(\hat{X}_k) = \frac{\hat{g}_n(\hat{X}_n) \varphi^*(0, \hat{X}_0)}{\varphi^*(n, \hat{X}_n)} = \varphi_n^*(0, \hat{X}_0) = Z_{dis}(\hat{X}_0).$$

□

A.3 Proof of Corollary 2.1

Proof. By definition,

$$Z_{dis}^{N, \varphi}(x) = \prod_{k=0}^n \frac{1}{N} \sum_{i=1}^N \hat{g}_k^{\varphi^*}(\zeta_k^i),$$

and

$$\begin{aligned}
\hat{g}_n^{\varphi^*}(x) &= \hat{g}_n(x) \ell_n^{\varphi^*}(x) = \frac{\hat{g}_n(x)}{\varphi^*(n, x)} \equiv 1, \\
\hat{g}_k^{\varphi^*}(x) &= \hat{g}_k(x) \ell_k^{\varphi^*}(x) = \hat{g}_k(x) \frac{\hat{P}[\varphi^*](k+1, x)}{\varphi^*(k, x)} \equiv 1, \quad 1 \leq k \leq n-1, \\
\hat{g}_0^{\varphi^*}(x) &= \hat{g}_0(x) \ell_0^{\varphi^*}(x) = \hat{g}_0(x) \hat{P}[\varphi^*](1, x) = \varphi^*(0, x).
\end{aligned}$$

Therefore,

$$Z_{dis}^{N, \varphi^*}(x) = \varphi^*(0, x) = Z_{dis}(x), \quad \forall x \in \mathbb{R}^d.$$

□

A.4 Proof of Proposition 2.3

Proof. 1. We first prove the Feynman-Kac representation formula. Fix $0 \leq t \leq T$, define the following process for $s \in [T-t, T]$

$$Y(s) := e^{\int_t^s h(\tau, X_\tau) d\tau} v^*(s, X_s).$$

Clearly,

$$Y(t) = v^*(t, X_t), \quad Y(T) = e^{\int_t^T h(\tau, X_\tau) d\tau} g(X_T).$$

By Itô's formula,

$$\begin{aligned} dY(s) &= e^{\int_t^s h(\tau, X_\tau) d\tau} h(s, X_s) v^*(s, X_s) ds \\ &\quad + e^{\int_t^s h(\tau, X_\tau) d\tau} \nabla_x v^*(s, X_s) \cdot (b(X_s) ds + \sqrt{2} dB_s) \\ &\quad + e^{\int_t^s h(\tau, X_\tau) d\tau} \Delta_x v^*(s, X_s) ds \\ &\quad + e^{\int_t^s h(\tau, X_\tau) d\tau} \partial_t v^*(s, X_s) ds \end{aligned}$$

By (2.23), we have

$$dY(s) = \sqrt{2} e^{\int_t^s h(\tau, X_\tau) d\tau} \nabla_x v^*(s, X_s) \cdot dB_s.$$

Hence, $Y(s)$ is a martingale, and consequently,

$$\mathbb{E}[Y(T) \mid X_t = x] = \mathbb{E}[Y(t) \mid X_t = x],$$

namely,

$$v^*(t, x) = \mathbb{E} \left[e^{\int_t^T h(\tau, X_\tau) d\tau} g(X_T) \mid X_t = x \right], \quad \forall x \in \mathbb{R}^d, \quad \forall t \in [0, T].$$

2. The existence and expression of the Radon-Nikodym derivative $L(T)$ is guaranteed by the classical Girsanov's theorem. We focus on the derivation of the zero-variance property (2.25) here.

For $s \in [0, T]$, define the process

$$\omega_s := e^{\int_0^s h(\tau, X_\tau^u) d\tau} v^*(s, X_s^u) L(s).$$

Clearly,

$$\omega_0 = v^*(0, X_0), \quad \omega_T = W.$$

By Itô's formula,

$$\begin{aligned} d\omega_s &= h(s, X_s^{u^*}) e^{\int_0^s h(\tau, X_\tau^u) d\tau} v^*(s, X_s^u) L(s) ds \\ &\quad + e^{\int_0^s h(\tau, X_\tau^u) d\tau} \partial_s v^*(s, X_s^{u^*}) L(s) ds \\ &\quad + e^{\int_0^s h(\tau, X_\tau^u) d\tau} \partial_x v^*(s, X_s^{u^*}) \cdot (b(X_s^{u^*}) ds + 2\partial_x \log v^*(s, X_s^{u^*}) ds + \sqrt{2} dB_s) L(s) \\ &\quad + e^{\int_0^s h(\tau, X_\tau^u) d\tau} v^*(s, X_s^{u^*}) L(s) (-\sqrt{2} \partial_x \log v^*(s, X_s^{u^*}) dB_s) \\ &\quad - e^{\int_0^s h(\tau, X_\tau^u) d\tau} L(s) (\sqrt{2} \partial_x v^*(s, X_s^{u^*}) \cdot \sqrt{2} \partial_x \log v^*(s, X_s^{u^*})) ds. \end{aligned}$$

Using the time evolution (2.23) for u^* , we have

$$d\omega_s \equiv 0.$$

Therefore

$$v^*(0, X_0) = \omega_0 = \omega_T = W \quad P^* - a.s.$$

□

B Proofs of Section 3

B.1 Proof of Proposition 3.1

Proof. Consider the following SDEs with the same initial state:

$$\begin{aligned} dX_t &= b(X_t)dt + \sqrt{2}dB, & X_0 &= x, & 0 \leq t \leq T = n\eta, \\ d\bar{X}_t &= b(\bar{X}_{k\eta})dt + \sqrt{2}dB, & \bar{X}_0 &= x, & t \in [k\eta, (k+1)\eta], & 0 \leq k \leq n-1. \end{aligned} \quad (\text{B.1})$$

Clearly, $P_\eta(x, \cdot) = \text{Law}(X_\eta)$ and $\hat{P}^\eta(x, \cdot) = \text{Law}(\bar{X}_\eta)$. Denote by $P_{[0,t]}^x, \hat{P}_{[0,t]}^x$ the path measures with the same initial x associated with the time interval $[0, t]$ for any fixed $t \leq T$. Then using the data processing inequality [2, 42] and Girsanov's theorem [21, 19], it holds that

$$\text{D}_{\text{KL}}(\text{Law}(\bar{X}_t) \parallel \text{Law}(X_t)) \leq \text{D}_{\text{KL}}(\hat{P}_{[0,t]}^x \parallel P_{[0,t]}^x) \leq \mathbb{E} \left[\sum_{k=0}^{\lceil t/\eta \rceil} \int_{k\eta}^{(k+1)\eta} |b(\bar{X}_t) - b(\bar{X}_{k\eta})|^2 dy \right]. \quad (\text{B.2})$$

By condition (a) in Assumption 3.1, $b(\cdot)$ is L_b -Lipschitz, and the second moment for $\bar{X}_{k\eta}$ has uniform bound, then for any $0 \leq k \leq \lceil t/\eta \rceil$, one has

$$\begin{aligned} \mathbb{E} |b(\bar{X}_t) - b(\bar{X}_{k\eta})|^2 &\leq L_b^2 \mathbb{E} \left| (t - k\eta)b(\bar{X}_{k\eta}) + \int_{k\eta}^t dB_s \right|^2 \\ &\leq 2L_b^2 \left(2\eta^2 \left(|b(0)|^2 + L_b^2 \sup_{0 \leq i \leq n} \mathbb{E} |\bar{X}_{i\eta}|^2 \right) + \eta d \right) \leq Cd\eta, \end{aligned} \quad (\text{B.3})$$

where we need $\eta < 1$ and $C = C(L_b, b(0), \sup_{0 \leq i \leq n} \mathbb{E} |\bar{X}_{i\eta}|^2)$ is a positive constant. Combining (B.2) and (B.3), we know that

$$\text{D}_{\text{KL}}(\text{Law}(\bar{X}_t) \parallel \text{Law}(X_t)) \leq Cd\eta.$$

And by Pinsker's inequality, we have

$$\text{TV}(\text{Law}(\bar{X}_t), \text{Law}(X_t)) \leq C\sqrt{d\eta}.$$

Finally, taking $t = \eta$, we obtain the desired result. \square

B.2 Proof of Proposition 3.2

Proof. Fix $T > 0, \eta > 0, x \in \mathbb{R}^d$. Recall that $T = n\eta$, and

$$\begin{aligned} Z_{dis}(x) &:= \mathbb{E}_x \left[\prod_{k=0}^{n-1} \hat{g}_k(\hat{X}_k) \hat{g}_n(\hat{X}_n) \right] = \mathbb{E}_x \left[\exp \left(\sum_{k=0}^{n-1} \int_{k\eta}^{(k+1)\eta} \log(\hat{g}_k(\hat{X}_k)) \eta^{-1} ds \right) \hat{g}_n(\hat{X}_n) \right], \\ Z_{con}(x) &= \mathbb{E}_x \left[e^{\int_0^T \log g(x, X_s) ds} g_T(X_T) \right]. \end{aligned}$$

Then, for

$$\begin{aligned} dX_t &= b(X_t)dt + \sqrt{2}dB, & X_0 &= x, & 0 \leq t \leq T = n\eta, \\ d\bar{X}_t &= b(\bar{X}_{k\eta})dt + \sqrt{2}dB, & \bar{X}_0 &= x, & t \in [k\eta, (k+1)\eta], & 0 \leq k \leq n-1, \end{aligned}$$

we have

$$\begin{aligned} &Z_{con}(x) - Z_{dis}(x) \\ &= \mathbb{E}_x \left[\exp \left(\int_0^T \log g(s, X_s) ds \right) g_T(X_T) \right] - \mathbb{E}_x \left[\exp \left(\int_0^T \log g(s, \bar{X}_s) ds \right) g_T(\bar{X}_T) \right] \\ &+ \mathbb{E}_x \left[\exp \left(\int_0^T \log g(s, \hat{X}_s) ds \right) (g_T(\bar{X}_T) - \hat{g}_n(\bar{X}_T)) \right] \\ &+ \mathbb{E}_x \left[\hat{g}_n(\bar{X}_T) \left(\prod_{i=0}^{n-1} \exp \left(\int_{i\eta}^{(i+1)\eta} \log g(s, \bar{X}_s) ds \right) - \prod_{i=0}^{n-1} \exp \left(\int_{i\eta}^{(i+1)\eta} \eta^{-1} \log \hat{g}_{i\eta}(\bar{X}_{i\eta}) ds \right) \right) \right], \end{aligned}$$

For the first term above, by condition (d) in Assumption 3.1, $\exp(\int_{k\eta}^T \log g(s, X_s) ds) g_T(X_T)$ is a continuous, bounded functional of $X_{[k\eta, T]}$ with $X_{k\eta} = x$, denote by $F_k(X_{[k\eta, T]})$. Then, using the KL upper bound for path measures obtained in (B.2), we have

$$\begin{aligned} & \mathbb{E}_x \left[\exp \left(\int_0^T \log g(s, X_s) ds \right) g_T(X_T) \right] - \mathbb{E}_x \left[\exp \left(\int_0^T \log g(s, \bar{X}_s) ds \right) g_T(\bar{X}_T) \right] \\ &= \mathbb{E}_x [F_0(X_{[0, T]})] - \mathbb{E}_x [F_0(\bar{X}_{[0, T]})] \\ &= \int F_0(y) (P_{[0, T]}^x(y) - \hat{P}_{[0, T]}^x(y)) dy \\ &\leq C \text{TV}(P_{[0, T]}^x, \hat{P}_{[0, T]}^x) \leq C \text{D}_{\text{KL}}(\hat{P}_{[0, T]}^x \| P_{[0, T]}^x)^{\frac{1}{2}} \leq C \sqrt{T d \eta} \rightarrow 0, \end{aligned}$$

where we have used the Pinsker's inequality in the last line above.

For the second term, by conditions (b), (d) in Assumption 3.1, $\exp(\int_0^T \log g(s, \hat{X}_s) ds)$ is bounded, and $\hat{g}_n(x) \rightarrow g_T(x)$ uniformly in x . Therefore, as $\eta \rightarrow 0$,

$$\mathbb{E}_x \left[\exp \left(\int_0^T \log g(s, \hat{X}_s) ds \right) (g_T(\bar{X}_T) - \hat{g}_n(\bar{X}_T)) \right] \rightarrow 0.$$

For the third term, for $s \in [i\eta, (i+1)\eta)$,

$$\begin{aligned} |\log g(s, \bar{X}_s) - \eta^{-1} \log \hat{g}_{i\eta}(\bar{X}_{i\eta})| &\leq |\log g(s, \bar{X}_s) - \log g(i\eta, \bar{X}_s)| \\ &\quad + |\log g(i\eta, \bar{X}_s) - \eta^{-1} \log \hat{g}_{i\eta}(\bar{X}_s)| + |\eta^{-1} \log \hat{g}_{i\eta}(\bar{X}_s) - \eta^{-1} \log \hat{g}_{i\eta}(\bar{X}_{i\eta})|. \end{aligned}$$

By conditions (b), (c) in Assumption 3.1, as $\eta \rightarrow 0$, $|\log g(s, x) - \log g(i\eta, x)|$, $|\log g(i\eta, x) - \eta^{-1} \log \hat{g}_{i\eta}(x)|$ tend to 0 uniformly in s, i, x . Moreover, by condition (c) in Assumption 3.1, $|\log \hat{g}_{i\eta}(\bar{X}_s) - \log \hat{g}_{i\eta}(\bar{X}_{i\eta})| \lesssim |\bar{X}_s - \bar{X}_{i\eta}| \lesssim \eta |b(\bar{X}_{i\eta})| + |W_s - W_{i\eta}|$. Hence, as $\eta \rightarrow 0$,

$$\mathbb{E}_x \left[\hat{g}_n(\bar{X}_T) \left(\prod_{i=0}^{n-1} \exp \left(\int_{i\eta}^{(i+1)\eta} \log g(s, \bar{X}_s) ds \right) - \prod_{i=0}^{n-1} \exp \left(\int_{i\eta}^{(i+1)\eta} \eta^{-1} \log \hat{g}_{i\eta}(\bar{X}_{i\eta}) ds \right) \right) \right] \rightarrow 0.$$

Combining all the above, we conclude that for any fixed $x \in \mathbb{R}^d$,

$$|Z_{dis}(x) - Z_{con}(x)| \rightarrow 0 \quad \text{as } \eta \rightarrow 0.$$

□

C Proof of Section 4

C.1 Proof of Lemma 4.1

Proof. We refer to [30] for a similar proof. The proof is based on the Jensen's inequality. In fact, by direct calculation and convexity of $-\log(\cdot)$, we have

$$\begin{aligned} -\log \mathbb{E}^{X \sim P} [\exp(-W(X))] &= -\log \int e^{-W(x)} P(dx) = -\log \int e^{-W(x)} \frac{dP}{dQ}(x) Q(dx) \\ &\leq \int \left(W(x) - \log \frac{dP}{dQ}(x) \right) Q(dx) = \mathbb{E}^{X \sim Q} [W(X)] + \text{D}_{\text{KL}}(Q \| P), \end{aligned}$$

and the equality holds if and only if

$$\frac{dQ}{dP}(X) = \exp(-\log \mathbb{E}^{X \sim P} [\exp(-W(X))] - W(X)).$$

□

C.2 Proof of Proposition 4.1

Proof. By definition (4.5), we have

$$\begin{aligned} J(\varphi) &= \mathbb{E}_x \left[- \sum_{k=0}^n \log \hat{g}_k(\hat{X}_k) \right] \\ &\quad + \int \log \left(\prod_{k=1}^n \frac{\varphi(k, x_k) \hat{P}(x_{k-1}, x_k)}{\hat{P}[\varphi](k, x_{k-1})} / \prod_{k=1}^n \hat{P}(x_{k-1}, x_k) \right) \prod_{k=1}^n \hat{P}_k^\varphi(x_{k-1}, x_k) dx_{1:n} \\ &= \mathbb{E}_x \left[- \sum_{k=0}^n \log \hat{g}_k(\hat{X}_k^\varphi) + \sum_{k=1}^n \log \frac{\varphi(k, \hat{X}_k^\varphi)}{\hat{P}[\varphi](k, X_{k-1}^\varphi)} \right], \end{aligned}$$

and

$$\begin{aligned} \text{D}_{\text{KL}}(P^\varphi \| P^{\varphi^*}) &= \int \log \left(\prod_{k=1}^n \frac{\varphi(k, x_k)}{\hat{P}[\varphi](k, x_{k-1})} / \prod_{k=1}^n \frac{\varphi^*(k, x_k)}{\hat{P}[\varphi^*](k, x_{k-1})} \right) \prod_{k=1}^n \hat{P}_k^\varphi(x_{k-1}, x_k) dx_{1:n} \\ &= \mathbb{E}_x \left[\sum_{k=1}^n \log \frac{\varphi(k, x_k)}{\hat{P}[\varphi](k, X_{k-1}^\varphi)} \right] - \int \log \left(\frac{\varphi^*(n, x_n)}{\varphi^*(0, x)} \prod_{k=0}^{n-1} \frac{\varphi^*(k, x_k)}{\hat{P}[\varphi^*](k+1, x_k)} \right) \prod_{k=1}^n \hat{P}_k^\varphi(x_{k-1}, x_k) dx_{1:n} \\ &= \mathbb{E}_x \left[- \sum_{k=0}^n \log \hat{g}_k(\hat{X}_k^\varphi) + \sum_{k=1}^n \log \frac{\varphi(k, \hat{X}_k^\varphi)}{\hat{P}[\varphi](k, X_{k-1}^\varphi)} \right] + \log \varphi_0^*(x), \end{aligned}$$

where we have used the recursive relation (2.11) in the last equality. Moreover, using the derived expression for $J(\varphi)$ and (2.11), we know that

$$J(\varphi^*) = \log \varphi_0^*(x).$$

Consequently,

$$J(\varphi) = J(\varphi^*) + \text{D}_{\text{KL}}(P^\varphi \| P^{\varphi^*}).$$

□

C.3 Proof of Proposition 4.2

Proof. The proof relies on the following auxiliary results:

- (Lemma C.1, generalized Jensen's inequality) Given deterministic functions $\phi : \Omega \rightarrow \mathbb{R}$ and $f : \mathbb{R} \rightarrow \mathbb{R}$. Assume that f is convex. Let λ, λ' be two probability measures on Ω that are absolutely continuous with each other. Define the functional

$$\mathcal{J}(f, \lambda, \phi) := \mathbb{E}_\lambda f(\phi) - f \mathbb{E}_\lambda \phi.$$

Then,

$$m \mathcal{J}(f, \lambda, \phi) \leq \mathcal{J}(f, \lambda', \phi) \leq M \mathcal{J}(f, \lambda, \phi), \quad (\text{C.1})$$

where $m := \inf_{E \in \mathcal{B}(\Omega)} \frac{\lambda'(E)}{\lambda(E)}$, $M := \sup_{E \in \mathcal{B}(\Omega)} \frac{\lambda(E)}{\lambda'(E)}$.

- (Lemma C.2, equivalence with the \mathcal{X}^2 -divergence)

$$r^2(\tilde{\nu}) = \mathcal{X}^2(\nu^* | \tilde{\nu}), \quad (\text{C.2})$$

where the \mathcal{X}^2 -divergence is defined by

$$\mathcal{X}^2(\nu^* | \tilde{\nu}) := \mathbb{E}_\mu \left[\left| \frac{d\nu^*}{d\tilde{\nu}} \right|^2 - 1 \right].$$

Now, by Jensen's inequality, we have

$$\mathrm{D}_{\mathrm{KL}}(\nu^* \|\tilde{\nu}) = \mathbb{E}_{\nu^*} \left[\log \frac{d\nu^*}{d\tilde{\nu}} \right] \leq \log \mathbb{E}_{\nu^*} \left[\frac{d\nu^*}{d\tilde{\nu}} \right] \quad (\text{C.3})$$

Combining (C.3) and (C.2), we have

$$r^2(\tilde{\nu}) = \mathcal{X}^2(\nu^* | \tilde{\nu}) = \mathbb{E}_{\mu} \left[\left| \frac{d\nu^*}{d\tilde{\nu}} \right|^2 - 1 \right] = \mathbb{E}_{\nu^*} \left[\frac{d\nu^*}{d\tilde{\nu}} \right] - 1 \geq e^{\mathrm{D}_{\mathrm{KL}}(\nu^* \|\tilde{\nu})} - 1.$$

For the second claim in Proposition 4.2, we choose $\lambda' = \nu^*$, $\lambda = \tilde{\nu}$, $\phi = \frac{d\nu^*}{d\tilde{\nu}}$, and $f = -\log$ in (C.1). Then,

$$\mathcal{J}(f, \lambda, \phi) = -\mathbb{E}_{\tilde{\nu}} \log \frac{d\nu^*}{d\tilde{\nu}} + \log \mathbb{E}_{\tilde{\nu}} \frac{d\nu^*}{d\tilde{\nu}} = \mathrm{D}_{\mathrm{KL}}(\tilde{\nu} \|\nu^*), \quad (\text{C.4})$$

and

$$\begin{aligned} \mathcal{J}(f, \lambda', \phi) &= -\mathbb{E}_{\nu^*} \log \frac{d\nu^*}{d\tilde{\nu}} + \log \mathbb{E}_{\nu^*} \frac{d\nu^*}{d\tilde{\nu}} \\ &= -\mathrm{D}_{\mathrm{KL}}(\nu^* \|\tilde{\nu}) + \log(\mathcal{X}^2(\nu^* | \tilde{\nu}) + 1) = -\mathrm{D}_{\mathrm{KL}}(\nu^* \|\tilde{\nu}) + \log(r^2(\tilde{\nu}) + 1), \end{aligned} \quad (\text{C.5})$$

where we have used (C.2) in the last equality. Combining (C.1), (C.4) and (C.5), we obtain the second claim

$$e^{m \mathrm{D}_{\mathrm{KL}}(\tilde{\nu} \|\nu^*) + \mathrm{D}_{\mathrm{KL}}(\nu^* \|\tilde{\nu})} - 1 \leq r^2(\tilde{\nu}) \leq e^{M \mathrm{D}_{\mathrm{KL}}(\tilde{\nu} \|\nu^*) + \mathrm{D}_{\mathrm{KL}}(\nu^* \|\tilde{\nu})} - 1,$$

where $m := \inf_E \frac{\nu^*(E)}{\tilde{\nu}(E)}$ and $M := \sup_E \frac{\nu^*(E)}{\tilde{\nu}(E)}$. \square

The two auxiliary lemmas used in the proof of Proposition 4.2 are given below:

Lemma C.1 (generalized Jensen's inequality). *Given deterministic functions $\phi : \Omega \rightarrow \mathbb{R}$ and $f : \mathbb{R} \rightarrow \mathbb{R}$. Assume that f is convex. Let λ, λ' be two probability measures on Ω that are absolutely continuous with each other. Define the functional*

$$\mathcal{J}(f, \lambda, \phi) := \mathbb{E}_{\lambda} f(\phi) - f(\mathbb{E}_{\lambda} \phi).$$

Then,

$$m \mathcal{J}(f, \lambda, \phi) \leq \mathcal{J}(f, \lambda', \phi) \leq M \mathcal{J}(f, \lambda, \phi), \quad (\text{C.6})$$

where $m := \inf_{E \in \mathcal{B}(\Omega)} \frac{\lambda'(E)}{\lambda(E)}$, $M := \inf_{E \in \mathcal{B}(\Omega)} \frac{\lambda(E)}{\lambda'(E)}$.

Proof. We first show that

$$m \mathcal{J}(f, \lambda, \phi) \leq \mathcal{J}(f, \lambda', \phi). \quad (\text{C.7})$$

Taking $E = \Omega$, we have

$$m := \inf_E \frac{\lambda'(E)}{\lambda(E)} \leq \frac{\lambda'(E)}{\lambda(E)} = 1.$$

Without loss of generosity, assume $m < 1$. (If $m = 1$, then $\lambda \equiv \lambda'$, and the argument is trivial). (C.7) is then equivalent to

$$m \mathbb{E}_{\lambda} f(\phi) - m f(\mathbb{E}_{\lambda} \phi) \leq \mathbb{E}_{\lambda'} f(\phi) - f(\mathbb{E}_{\lambda'} \phi). \quad (\text{C.8})$$

Since $m \in (0, 1)$, and $m = \inf_E \frac{\lambda'(E)}{\lambda(E)}$, the probability $\bar{\lambda} := \frac{\lambda' - m\lambda}{1-m}$ is well-defined. Then, by Jensen's inequality, since f is convex, we have

$$\mathbb{E}_{\lambda'} f(\phi) - m \mathbb{E}_{\lambda} f(\phi) = (1-m) \mathbb{E}_{\bar{\lambda}} f(\phi) \geq (1-m) f(\mathbb{E}_{\bar{\lambda}} \phi) = (1-m) f\left(\frac{\mathbb{E}_{\lambda'} \phi - m \mathbb{E}_{\lambda} \phi}{1-m}\right).$$

Using convexity of f again, we have

$$(1-m) f\left(\frac{\mathbb{E}_{\lambda'} \phi - m \mathbb{E}_{\lambda} \phi}{1-m}\right) + m f(\mathbb{E}_{\lambda} \phi) \geq f(\mathbb{E}_{\lambda'} \phi).$$

Therefore, (C.8) holds, and thus

$$m\mathcal{J}(f, \lambda, \phi) \leq \mathcal{J}(f, \lambda', \phi).$$

Assuming $M > 1$ and using exactly the same arguments, we have

$$M\mathcal{J}(f, \lambda, \phi) \geq \mathcal{J}(f, \lambda', \phi).$$

□

Lemma C.2. *Recall the definitions of $\tilde{\nu}$, ν^* and the relative variance $r(\tilde{\nu})$ in Proposition 4.2. Then*

$$r^2(\tilde{\nu}) = \mathcal{X}^2(\nu^*|\tilde{\nu}), \tag{C.9}$$

where the \mathcal{X}^2 -divergence is defined by

$$\mathcal{X}^2(\nu^*|\tilde{\nu}) := \mathbb{E}_\mu \left[\left| \frac{d\nu^*}{d\tilde{\nu}} \right|^2 - 1 \right].$$

Proof. By definition, we have

$$\mathcal{X}^2(\nu^*|\tilde{\nu}) := \mathbb{E}_\mu \left[\left| \frac{d\nu^*}{d\tilde{\nu}} \right|^2 - 1 \right] = \mathbb{E}_{\tilde{\nu}} \left| \frac{d\nu^*}{d\tilde{\nu}} \right|^2 - \left| \mathbb{E}_{\tilde{\nu}} \frac{d\nu^*}{d\tilde{\nu}} \right|^2 = \text{Var}_{\tilde{\nu}} \left(\frac{d\nu^*}{d\tilde{\nu}} \right) = \text{Var}_{\tilde{\nu}} \left(\frac{d\nu^*}{d\nu} \frac{d\nu}{d\tilde{\nu}} \right).$$

Recall the zero-variance property of ν^* :

$$\frac{d\nu^*}{d\nu} = \frac{e^{-W}}{Z} \quad \nu - a.s..$$

Consequently,

$$\text{Var}_{\tilde{\nu}} \left(\frac{d\nu^*}{d\nu} \frac{d\nu}{d\tilde{\nu}} \right) = \text{Var}_{\tilde{\nu}} \left(\frac{e^{-W}}{Z} \frac{d\nu}{d\tilde{\nu}} \right) = \frac{\text{Var}_{\tilde{\nu}} \left(e^{-W} \frac{d\nu}{d\tilde{\nu}} \right)}{Z^2} = r^2(\tilde{\nu}).$$

Hence,

$$r^2(\tilde{\nu}) = \mathcal{X}^2(\nu^*|\tilde{\nu}).$$

□

References

- [1] Hernan P Awad, Peter W Glynn, and Reuven Y Rubinstein. Zero-variance importance sampling estimators for Markov process expectations. *Mathematics of Operations Research*, 38(2):358–388, 2013.
- [2] Normand J Beaudry and Renato Renner. An intuitive proof of the data processing inequality. *arXiv preprint arXiv:1107.0740*, 2011.
- [3] Joshua J Bon, Christopher Drovandi, and Anthony Lee. Monte Carlo twisting for particle filters. *arXiv preprint arXiv:2208.04288*, 2022.
- [4] Michelle Boué and Paul Dupuis. A variational representation for certain functionals of Brownian motion. *The Annals of Probability*, 26(4):1641–1659, 1998.
- [5] Nicola Branchini and Víctor Elvira. Optimized auxiliary particle filters: adapting mixture proposals via convex optimization. In *Uncertainty in Artificial Intelligence*, pages 1289–1299. PMLR, 2021.
- [6] Nicolas Chopin. A sequential particle filter method for static models. *Biometrika*, 89(3):539–552, 2002.

- [7] George Cybenko. Approximation by superpositions of a sigmoidal function. *Mathematics of control, signals and systems*, 2(4):303–314, 1989.
- [8] Arnak S Dalalyan. Theoretical guarantees for approximate sampling from smooth and log-concave densities. *Journal of the Royal Statistical Society Series B: Statistical Methodology*, 79(3):651–676, 2017.
- [9] Pierre Del Moral. *Feynman-Kac formulae*. Springer, 2004.
- [10] Pierre Del Moral, Arnaud Doucet, and Ajay Jasra. Sequential Monte Carlo samplers. *Journal of the Royal Statistical Society Series B: Statistical Methodology*, 68(3):411–436, 2006.
- [11] Pierre Del Moral, Arnaud Doucet, and Ajay Jasra. On adaptive resampling strategies for sequential Monte Carlo methods. *Bernoulli*, 18(1):252–278, 2012.
- [12] Jean-Dominique Deuschel and Daniel W Stroock. *Large deviations*, volume 342. American Mathematical Soc., 2001.
- [13] Petar M Djuric, Jayesh H Kotecha, Jianqui Zhang, Yufei Huang, Tadesse Ghirmai, Mónica F Bugallo, and Joaquin Miguez. Particle filtering. *IEEE signal processing magazine*, 20(5):19–38, 2003.
- [14] Arnaud Doucet, Nando De Freitas, and Neil Gordon. An introduction to sequential Monte Carlo methods. *Sequential Monte Carlo methods in practice*, pages 3–14, 2001.
- [15] Arnaud Doucet, Simon Godsill, and Christophe Andrieu. On sequential Monte Carlo sampling methods for Bayesian filtering. *Statistics and computing*, 10:197–208, 2000.
- [16] Arnaud Doucet, Adam M Johansen, et al. A tutorial on particle filtering and smoothing: Fifteen years later. *Handbook of nonlinear filtering*, 12(656-704):3, 2009.
- [17] Kenji Doya. Temporal difference learning in continuous time and space. *Advances in neural information processing systems*, 8, 1995.
- [18] James Durbin and Siem Jan Koopman. *Time series analysis by state space methods*, volume 38. OUP Oxford, 2012.
- [19] Richard Durrett. *Stochastic calculus: a practical introduction*. CRC press, 2018.
- [20] Marco Fuhrman, Federica Masiero, and Gianmario Tessitore. Stochastic equations with delay: Optimal control via BSDEs and regular solutions of Hamilton-Jacobi-Bellman equations. *SIAM Journal on Control and Optimization*, 48(7):4624–4651, 2010.
- [21] Igor Vladimirovich Girsanov. On transforming a certain class of stochastic processes by absolutely continuous substitution of measures. *Theory of Probability & Its Applications*, 5(3):285–301, 1960.
- [22] Paul Glasserman. *Monte Carlo methods in financial engineering*, volume 53. Springer, 2004.
- [23] Paul Glasserman and Jingyi Li. Importance sampling for portfolio credit risk. *Management science*, 51(11):1643–1656, 2005.
- [24] Peter W Glynn and Donald L Iglehart. Importance sampling for stochastic simulations. *Management science*, 35(11):1367–1392, 1989.
- [25] Neil J Gordon, David J Salmond, and Adrian FM Smith. Novel approach to nonlinear/non-Gaussian Bayesian state estimation. In *IEE proceedings F (radar and signal processing)*, volume 140, pages 107–113. IET, 1993.

- [26] Pieralberto Guarniero, Adam M Johansen, and Anthony Lee. The iterated auxiliary particle filter. *Journal of the American Statistical Association*, 112(520):1636–1647, 2017.
- [27] Tuomas Haarnoja, Haoran Tang, Pieter Abbeel, and Sergey Levine. Reinforcement learning with deep energy-based policies. In *International conference on machine learning*, pages 1352–1361. PMLR, 2017.
- [28] Jiequn Han, Arnulf Jentzen, and Weinan E. Solving high-dimensional partial differential equations using deep learning. *Proceedings of the National Academy of Sciences*, 115(34):8505–8510, 2018.
- [29] Carsten Hartmann and Lorenz Richter. Nonasymptotic bounds for suboptimal importance sampling. *SIAM/ASA Journal on Uncertainty Quantification*, 12(2):309–346, 2024.
- [30] Carsten Hartmann, Lorenz Richter, Christof Schütte, and Wei Zhang. Variational characterization of free energy: Theory and algorithms. *Entropy*, 19(11):626, 2017.
- [31] Carsten Hartmann and Christof Schütte. Efficient rare event simulation by optimal nonequilibrium forcing. *Journal of Statistical Mechanics: Theory and Experiment*, 2012(11):P11004, 2012.
- [32] Carsten Hartmann, Christof Schütte, and Wei Zhang. Model reduction algorithms for optimal control and importance sampling of diffusions. *Nonlinearity*, 29(8):2298, 2016.
- [33] Jeremy Heng, Adrian N Bishop, George Deligiannidis, and Arnaud Doucet. Controlled sequential Monte Carlo. *The Annals of Statistics*, 48(5):2904–2929, 2020.
- [34] Forrest Iandola, Matt Moskewicz, Sergey Karayev, Ross Girshick, Trevor Darrell, and Kurt Keutzer. Densenet: Implementing efficient convnet descriptor pyramids. *arXiv preprint arXiv:1404.1869*, 2014.
- [35] Rudolph Emil Kalman. A new approach to linear filtering and prediction problems. 1960.
- [36] Omar Kebiri, Lara Neureither, and Carsten Hartmann. Adaptive importance sampling with forward-backward stochastic differential equations. In *Stochastic Dynamics Out of Equilibrium: Institut Henri Poincaré, Paris, France, 2017*, pages 265–281. Springer, 2019.
- [37] Genshiro Kitagawa. Monte Carlo filter and smoother for non-Gaussian nonlinear state space models. *Journal of computational and graphical statistics*, 5(1):1–25, 1996.
- [38] Teun Kloek and Herman K Van Dijk. Bayesian estimates of equation system parameters: an application of integration by Monte Carlo. *Econometrica: Journal of the Econometric Society*, pages 1–19, 1978.
- [39] Augustine Kong, Jun S Liu, and Wing Hung Wong. Sequential imputations and Bayesian missing data problems. *Journal of the American statistical association*, 89(425):278–288, 1994.
- [40] Dieterich Lawson, Allan Raventós, Andrew Warrington, and Scott Linderman. Sixo: Smoothing inference with twisted objectives. *Advances in Neural Information Processing Systems*, 35:38844–38858, 2022.
- [41] Dieterich Lawson, George Tucker, Christian A Naesseth, Chris Maddison, Ryan P Adams, and Yee Whye Teh. Twisted variational sequential Monte Carlo. In *Third workshop on Bayesian Deep Learning (NeurIPS)*, 2018.
- [42] Lei Li, Yuelin Wang, and Yuliang Wang. Propagation of chaos in path spaces via information theory. *arXiv preprint arXiv:2312.00339*, 2023.

- [43] Lei Li and Yuliang Wang. A sharp uniform-in-time error estimate for Stochastic Gradient Langevin Dynamics. *arXiv preprint arXiv:2207.09304*, 2022.
- [44] Han Cheng Lie. *On a strongly convex approximation of a stochastic optimal control problem for importance sampling of metastable diffusions*. PhD thesis, 2016.
- [45] Jun S Liu and Rong Chen. Blind deconvolution via sequential imputations. *Journal of the american statistical association*, 90(430):567–576, 1995.
- [46] Jun S Liu and Rong Chen. Sequential Monte Carlo methods for dynamic systems. *Journal of the American statistical association*, 93(443):1032–1044, 1998.
- [47] Edward N Lorenz. Predictability: A problem partly solved. In *Proc. Seminar on predictability*, volume 1. Reading, 1996.
- [48] Wenlong Mou, Nicolas Flammarion, Martin J Wainwright, and Peter L Bartlett. Improved bounds for discretization of Langevin diffusions: Near-optimal rates without convexity. *Bernoulli*, 28(3):1577–1601, 2022.
- [49] Wenlong Mou and Yuhua Zhu. On Bellman equations for continuous-time policy evaluation i: discretization and approximation. *arXiv preprint arXiv:2407.05966*, 2024.
- [50] Lawrence M Murray, Sumeetpal S Singh, and Anthony Lee. Anytime Monte Carlo. *Data-Centric Engineering*, 2:e7, 2021.
- [51] M Netto, L Gimeno, and M Mendes. On the optimal and suboptimal nonlinear filtering problem for discrete-time systems. *IEEE Transactions on Automatic Control*, 23(6):1062–1067, 1978.
- [52] Michael K Pitt and Neil Shephard. Filtering via simulation: Auxiliary particle filters. *Journal of the American statistical association*, 94(446):590–599, 1999.
- [53] Enric Ribera Borrell, Jannes Quer, Lorenz Richter, and Christof Schütte. Improving control based importance sampling strategies for metastable diffusions via adapted metadynamics. *SIAM Journal on Scientific Computing*, 46(2):S298–S323, 2024.
- [54] Lorenz Richter. *Solving high-dimensional PDEs, approximation of path space measures and importance sampling of diffusions*. PhD thesis, BTU Cottbus-Senftenberg, 2021.
- [55] Simo Särkkä and Lennart Svensson. *Bayesian filtering and smoothing*, volume 17. Cambridge university press, 2023.
- [56] John Schulman, Xi Chen, and Pieter Abbeel. Equivalence between policy gradients and soft q-learning. *arXiv preprint arXiv:1704.06440*, 2017.
- [57] Nisan Stiennon, Long Ouyang, Jeffrey Wu, Daniel Ziegler, Ryan Lowe, Chelsea Voss, Alec Radford, Dario Amodei, and Paul F Christiano. Learning to summarize with human feedback. *Advances in Neural Information Processing Systems*, 33:3008–3021, 2020.
- [58] Richard S Sutton. Learning to predict by the methods of temporal differences. *Machine learning*, 3:9–44, 1988.
- [59] Richard S Sutton, David McAllester, Satinder Singh, and Yishay Mansour. Policy gradient methods for reinforcement learning with function approximation. *Advances in neural information processing systems*, 12, 1999.
- [60] Guangchen Wang, Zhen Wu, Jie Xiong, et al. *An introduction to optimal control of FBSDE with incomplete information*. Springer, 2018.
- [61] Haoran Wang, Thaleia Zariphopoulou, and Xun Yu Zhou. Reinforcement learning in continuous time and space: A stochastic control approach. *Journal of Machine Learning Research*, 21(198):1–34, 2020.

- [62] Mike West. Mixture models, Monte Carlo, Bayesian updating, and dynamic models. *Computing Science and Statistics*, pages 325–325, 1993.
- [63] Nick Whiteley and Anthony Lee. Twisted particle filters. *The Annals of Statistics*, 42(1):115–141, 2014.
- [64] Ronald J Williams. Simple statistical gradient-following algorithms for connectionist reinforcement learning. *Machine learning*, 8:229–256, 1992.
- [65] Kevin Yang and Dan Klein. FUDGE: Controlled text generation with future discriminators. In *Proceedings of the 2021 Conference of the North American Chapter of the Association for Computational Linguistics: Human Language Technologies*, pages 3511–3535, 2021.
- [66] Wei Zhang, Han Wang, Carsten Hartmann, Marcus Weber, and Christof Schütte. Applications of the cross-entropy method to importance sampling and optimal control of diffusions. *SIAM Journal on Scientific Computing*, 36(6):A2654–A2672, 2014.
- [67] Stephen Zhao, Rob Brekelmans, Alireza Makhzani, and Roger Grosse. Probabilistic inference in language models via twisted sequential Monte Carlo. *arXiv preprint arXiv:2404.17546*, 2024.
- [68] Mo Zhou and Jianfeng Lu. Solving time-continuous stochastic optimal control problems: Algorithm design and convergence analysis of actor-critic flow. *arXiv preprint arXiv:2402.17208*, 2024.
- [69] Daniel M Ziegler, Nisan Stiennon, Jeffrey Wu, Tom B Brown, Alec Radford, Dario Amodei, Paul Christiano, and Geoffrey Irving. Fine-tuning language models from human preferences. *arXiv preprint arXiv:1909.08593*, 2019.
- [70] Andy Zou, Zifan Wang, J Zico Kolter, and Matt Fredrikson. Universal and transferable adversarial attacks on aligned language models. *arXiv preprint arXiv:2307.15043*, 2023.